Contribution of Tropical Cyclones to the North Atlantic Climatological Rainfall as Observed from Satellites

Edward B. Rodgers*, Robert F. Adler[1], And Harold F. Pierce[2]

(1) Laboratory for Atmospheres, NASA/Goddard Space Flight Center, Greenbelt, MD 20771

2. Science Systems and Applications Inc. Lanham, MD 20706

* Deceased

June 2000

Submitted to *Journal of Applied Meteorology*

Corresponding author address: Dr Robert F. Adler, Mesoscale Atmosphere Processes Branch (Code 912) Laboratory for Atmospheres, NASA/ Goddard Space Flight Center, Greenbelt MD 20771 Email address: adler@agnes.gsfc.nasa.gov

Abstract

The tropical cyclone rainfall climatology study that was performed for the North Pacific (Rodgers et al. 2000) was extended to the North Atlantic. Similar to the North Pacific tropical cyclone study, mean monthly rainfall within 444 km of the center of the North Atlantic tropical cyclones (ie., that reached storm stage and greater) was estimated from passive microwave satellite observations during an eleven year period. These satellite-observed rainfall estimates were used to assess the impact of tropical cyclone rainfall in altering the geographical, seasonal, and inter-annual distribution of the North Atlantic total rainfall during June-November when tropical cyclones were most abundant.

The main results from this study indicate: 1) that tropical cyclones contribute, respectively, 4%, 3%, and 4% to the western, eastern, and entire North Atlantic; 2) similar to that observed in the North Pacific, the maximum in North Atlantic tropical cyclone rainfall is approximately 5-10° poleward (depending on longitude) of the maximum non-tropical cyclone rainfall; 3) tropical cyclones contribute regionally a maximum of 30% of the total rainfall northeast of Puerto Rico, within a region near 15° N 55° W, and off the west coast of Africa; 4) there is no lag between the months with maximum tropical cyclone rainfall and non-tropical cyclone rainfall in the western North Atlantic, while in the eastern North Atlantic, maximum tropical cyclone rainfall precedes maximum non-tropical cyclone rainfall; 5) like the North Pacific, North Atlantic tropical cyclones of hurricane intensity generate the greatest amount of rainfall in the higher latitudes; and 6) warm ENSO events inhibit tropical cyclone rainfall.

Contribution of Tropical Cyclones to the North Atlantic Climatological Rainfall as Observed from Satellites

Edward B. Rodgers*, Robert F. Adler[1], And Harold F. Pierce[2]

(1) Laboratory for Atmospheres, NASA/Goddard Space Flight Center, Greenbelt, MD 20771

2. Science Systems and Applications Inc. Lanham, MD 20706

* Deceased

June 2000

Submitted to *Journal of Applied Meteorology*

Corresponding author address: Dr Robert F. Adler, Mesoscale Atmosphere Processes Branch (Code 912) Laboratory for Atmospheres, NASA/ Goddard Space Flight Center, Greenbelt MD 20771 Email address: adler@agnes.gsfc.nasa.gov

Abstract

The tropical cyclone rainfall climatology study that was performed for the North Pacific (Rodgers et al. 2000) was extended to the North Atlantic. Similar to the North Pacific tropical cyclone study, mean monthly rainfall within 444 km of the center of the North Atlantic tropical cyclones (ie., that reached storm stage and greater) was estimated from passive microwave satellite observations during an eleven year period. These satellite-observed rainfall estimates were used to assess the impact of tropical cyclone rainfall in altering the geographical, seasonal, and inter-annual distribution of the North Atlantic total rainfall during June-November when tropical cyclones were most abundant.

The main results from this study indicate: 1) that tropical cyclones contribute, respectively, 4%, 3%, and 4% to the western, eastern, and entire North Atlantic; 2) similar to that observed in the North Pacific, the maximum in North Atlantic tropical cyclone rainfall is approximately 5-10° poleward (depending on longitude) of the maximum non-tropical cyclone rainfall; 3) tropical cyclones contribute regionally a maximum of 30% of the total rainfall northeast of Puerto Rico, within a region near 15° N 55° W, and off the west coast of Africa; 4) there is no lag between the months with maximum tropical cyclone rainfall and non-tropical cyclone rainfall in the western North Atlantic, while in the eastern North Atlantic, maximum tropical cyclone rainfall precedes maximum non-tropical cyclone rainfall; 5) like the North Pacific, North Atlantic tropical cyclones of hurricane intensity generate the greatest amount of rainfall in the higher latitudes; and 6) warm ENSO events inhibit tropical cyclone rainfall.

1. Introduction

One of the main driving forces for the motion of the earth's atmosphere is provided by tropical heat sources generated by the combination of clouds and precipitation. An important source of rainfall for agriculture and other water applications over the regions of the subtropics and tropics is tropical cyclones. However, questions remain concerning the amount that tropical cyclones contribute to the total (i.e., combined tropical and non-tropical cyclone rainfall) rainfall, how these tropical cyclone rainfall patterns are distributed geographically and seasonally, and how climate variations such as ENSO events affect tropical cyclone rainfall.

Using passive microwave satellite observations, these questions have been addressed by Rodgers et. al. (2000) for the North Pacific for the years of 1987-1998 during the tropical cyclone season (i.e., June- November) with the following results. Tropical cyclones contribute approximately 7% of the rainfall in the entire domain of the North Pacific during a tropical cyclone season, with maximum regional contributions of approximately 30% northeast of the Philippines Islands and 40% off the lower Baja California coast. It has also been shown that tropical cyclone rainfall in the western North Pacific is affected significantly by ENSO variations in the opposite sense of what might be expected. For example, during the El Niño events that occurred during these years, high sea surface temperatures (SSTs) and evaporation are produced that create more total precipitation than normal in the eastern and central North Pacific. Moreover, the El Niño years produce lower than normal SSTs and non-tropical cyclone precipitation

in the western North Pacific. However, tropical cyclone rainfall amounts in the western North Pacific are greater than normal despite the lower SSTs due to the El Niño induced lower-tropospheric circulation patterns that are favorable for tropical cyclone genesis and intensification.

The next question that should be addressed is the manner in which tropical cyclones influence the distribution of total **North Atlantic** rainfall. In this study, monthly North Atlantic tropical cyclone rainfall and the rainfall generated by all other North Atlantic systems are determined using data from the Special Sensor Microwave/Imager (SSM/I) instrument on board the Defense Meteorological Satellite Program (DMSP) satellites. The SSM/I observations are collected over the North Atlantic domain (0°-35° N by 0°-100°W) during the months of June–November when tropical cyclones are most abundant for the years 1987-1989 and 1991-1998 (there was little SSM/I data available during 1990). These monthly rainfall observations are then used to examine geographical, seasonal, and inter-annual variations in North Atlantic tropical cyclone rainfall.

2 Data Analyses

a Special Sensor Microwave/Radiometer (SSM/I)

The DMSP satellites circle the globe 14.1 times per day along a near sun-synchronous orbit at an altitude of 833 km and a 98.8° inclination. The SSM/I sensors on

board DMSP F-8, F-10. F-11, F-13, and F-14 satellites measure reflected and emitted dual polarized microwave radiation at frequencies of 19.4, 37.0, and 85.5 GHz and vertically polarized microwave radiation at 22.2 GHz. The SSM/I scan conically at a 45° angle from nadir and have an observational swath width of approximately 1400 km at the earth's surface. The F-8 DMSP SSM/I was fully operational from the first week of July 1987 to February 1990, while the F-10 DMSP SSM/I was partially operational from December 1990 to January 1992 and fully operation thereafter. The F-11 DMSP SSM/I had been fully operational since January 1992, while the F-13 and F-14 DMSP SSM/Is were, respectively, launched in May 1995 and May 1996 and has been fully operational ever since. The ascending (descending) F-8, F-10, F-11, F-13, and F-14 DMSP orbits, respectively, cross the equator near the eastern North Pacific at approximately 00:20 (11:50). 04:05 (16:30), 01:34 (13:08), 23:35 (12:08), and 01:47 (14:29) UTC. Further information concerning the SSM/I sensor measurements and orbital mechanics can be found in Hollinger et al. (1991).

b SSM/I brightness temperature-rainrate algorithm

Rainrates are obtained from the SSM/I-derived brightness temperatures by utilizing an algorithm developed by Adler et. al. (1994). The algorithm is called the Version 2 Goddard Scattering Algorithm (GSCAT-2). The algorithm uses a combination of the 37.0, 22.2, and 19.9 GHz channels to define potential raining regions over the ocean and the 85.5 GHz channel to derive rainrates greater than 1 mm h^{-1} within the raining areas. Both the rain criteria and the rainrate and the brightness temperature

relationship are based on cloud model calculations (Adler et. al. 1991). The algorithm is chosen for its computational simplicity and its enhanced instantaneous field of view (IFOV) in observing rainrates from the 85.5 GHz channel (i.e., 15 by 15 km). Areal mean rainrates derived from SSM/I for the inner core (i.e., within 111 km of the tropical cyclone center) of the 1987-1989 western North Atlantic tropical cyclones using the GSCAT-2 algorithm are found (see Table 2 in Rodgers et al., 1994) to compare favorably with most of the early estimates that are obtained from rain gages, water vapor budget studies, and earlier satellite-based microwave observations.

c Sampling Technique

To assemble the mean monthly tropical cyclone rainfall data, SSM/I-derived tropical cyclone rainrates are used. Only the rainrates that are observed within 444 km radius of the center of circulation of North Atlantic tropical cyclones by SSM/I are sampled. This tropical cyclone rainrate sampling area is chosen to encompass the majority of the rainfall that is contributed by tropical cyclones, which includes the eye wall and the inner and outer rain bands. The center of the sampled tropical cyclones for the time of the SSM/I passes are extrapolated from the best track data.

Within the 444 km circular domain, the SSM/I sensors were able to monitor the rainrates at least once for 136 western and 111 eastern North Atlantic tropical cyclones The sample does not include tropical cyclones that never reached storm stage. From these observations, the SSM/I tropical cyclone rainrate samples include 38 depressions, 57 storms (18-31 ms^{-1}), 36 hurricanes (32-62 m s^{-1}) and 1 super hurricane (> 62 m s^{-1}) in

the western North Atlantic and 33 depressions, 51 storms, 26 hurricanes, and 1 super hurricane in the eastern North Atlantic Moreover, for tropical cyclones that occur over land, the SSM/I-derived rainrates are only sampled for dissipating tropical cyclones that are followed by the best track reports. Therefore, for these reasons the study will slightly underestimate the total tropical cyclone rainfall.

The analysis area for this study covers both land water regions of the North Atlantic that is divided into two regions. The western North Atlantic region is located between 0°-35° N and 50°-100° W, while the eastern North Atlantic area of analyses is located between 0°-35° N and 0°-50° W (see Fig. 1). In the western region, the eastern North Pacific tropical cyclone rainfall is eliminated from the sample by deleting the tropical cyclones in that region, while non-tropical cyclone rainfall is kept. The two North Atlantic domains are arbitrarily chosen in order to partition the ocean basins into equal geographical areas. The domain was also chosen to eliminate regions of the North Atlantic near the equator where tropical cyclones are rarely observed due to limited coriolis forcing (i.e., latitudes less than 5° N) or at high latitudes due to strong vertical wind shear that is greater than 10 ms^{-1} and/or SSTs less than 26° C (i.e., latitudes greater than 35° N).

To estimate the monthly tropical cyclone rainfall the SSM/I-derived rainrates that are sampled within 444 km of the center of each tropical cyclones are accumulated and averaged for a 2.5° latitudinal/longitudinal grid and then multiplied by the number of

hours for a given month using equation 1 found in Rodgers et al. (2000). These values will be referred to as "**tropical cyclone rainfall**" in the remaining portion of the text.

The total rainfall from all systems is then calculated considering all SSM/I observations and will be referred to as "**total rainfall**" in the remaining portion of the text. Finally, the non-tropical cyclone rainfall is calculated from the differences between the total rainfall and that estimated from tropical cyclones and will be referred to as "**non-tropical cyclone rainfall**" in the remaining portion of the text.

In order to make the SSM/I observations more homogeneous from year to year and from month to month, the following adjustments in the SSM/I-derived mean rainfall data sets are made. First, the accumulated monthly rainfall amounts for the inter-annual rainfall analyses are generated from a single SSM/I satellite from 1992-1998 when multiple SSM/Is were flown. For the other rainfall analyses all available SSM/Is data are used. Second, since the DMSP F-8 SSM/I was not operational until after June 1987 and during the tropical cyclone season of 1990, the mean inter-annual rainfall set was limited to months of July- November. In addition, the mean seasonal rainfall analyses for the months of June-November only contained the years of 1988-1989 and 1991- 1998 (e.g. total of 60 months).

d Sea Surface Temperatures (SST)

To examine the variation of SSTs during the El Niño and La Niña years during this 10 year period, global mean monthly SSTs for a given year were used. The month of September was chosen since it is the month with the maximum tropical cyclone occurrences. These SSTs were provided by the National Meteorological Center and averaged for a 2.5° latitudinal/longitudinal horizontal grid (Reynolds and Smith 1994).

3. Results

a Geographical distribution of non-tropical cyclone and tropical cyclone rainfall

The upper, middle, and lower panels of Fig. 2 show, respectively, the geographical distribution of mean monthly non-tropical cyclone rainfall, the mean tropical cyclone rainfall, and the percentage of rainfall contributed by tropical cyclones (i.e., the ratio of tropical cyclone rainfall to total rainfall) over the North Atlantic during the 65 month period. The upper panel of Fig. 2 indicates that the region with the greatest non-tropical cyclone rainfall amount (i.e., greater than 300 mm month^{-1}) is associated with the ascending branch of the Hadley circulation that helps to maintain the ITCZ regions and the active baroclinic zone off the east coast of United States. Regions of moderate non-tropical cyclone rainfall amounts (i.e., 200-300 mm month^{-1}) appear to be associated with the baroclinic zone that extends northward and southeastward into the western Caribbean Sea and the Gulf of Mexico. Finally, regions of light non-tropical cyclone rainfall amounts (less than 200 mm month^{-1}) appear to be associated with the descending branch of the Hadley circulation over vast regions of the subtropics, Northern

Africa, Southern Spain, and the east and southeastern United States. It is noted that the dry region over the eastern region of the North Atlantic extends southwestward towards the region between Puerto Rico and the coast of Venezuela and Columbia. The dry atmosphere is manifested by persistent divergent lower-tropospheric flow. The non-tropical cyclone mean monthly rainfall amounts for the 65 month period are found to be, respectively, 209, 123, and 166 mm month^{-1} for the western, eastern, and the entire North Atlantic. The North Atlantic mean monthly rainfall amounts are somewhat less than that found in the North Pacific for the same time period.

The middle panel of Fig. 2, suggests that the maximum tropical cyclone rainfall is concentrated in the subtropical latitudes from the middle North Atlantic west towards the Gulf of Mexico. No tropical cyclone rainfall is found off the west coast of Spain and Africa and equatorward of 5° N latitude. The regional area with the greatest tropical cyclone rainfall (i.e., greater than 30 mm month^{-1}) occurs east of Puerto Rico and north of the Lesser Antilles. This is the region where many tropical cyclones during the period recurved and momentarily intensified. The mean monthly rainfall contributed by tropical cyclones during the period are, respectively 9, 3, and 6 mm month^{-1} for the western, eastern, and entire North Atlantic domain.

Comparing the middle and upper panels of Fig. 2, it can be seen that, like the North Pacific (Rodgers et al 2000), the maximum North Atlantic tropical cyclone rainfall is slightly poleward of the maximum non-tropical cyclone rainfall found in the ITCZ. This is especially obvious in the percentage fields seen in the lower panel of Fig. 2. It

can be seen that the regions where tropical cyclones contribute the greatest rainfall are in the dry regions of the subtropics north and west of the ITCZ. For example, northeast of Puerto Rico where the non-tropical cyclone rainfall for this period is less than 150 mm month^{-1}, the area receives more than 30% additional rainfall from tropical cyclones. Thus, it appears that without the presence of the tropical cyclones that Puerto Rico endured, rainfall during their growing season would be limited. Fig. 2 also indicates that tropical cyclones contributed as much as 10% to the total rainfall over land areas of the Southeastern United States, Yucatan Peninsula, and Central America. However, it should be reemphasized that tropical cyclone rainfall over land and along coastal regions may be underestimated in this study for the reasons given in section 2. Also, shallow orographic rainfall that is confined primarily below the freezing level may be missed or underestimated by the GSCAT technique that is dependent on scattering due to ice in order to estimate precipitation. The mean percentage of rainfall contributed by tropical cyclones during this period for the western, eastern, and entire North Atlantic are, respectively, 4%, 3%, and 4%.

Zonally averaged non-tropical cyclone and tropical cyclone profiles for both the western and eastern North Atlantic are seen in Fig. 3. In the western North Atlantic (Fig. 3a), there is a broad zonal region of high tropical cyclone rainfall amounts (>10 mm month^{-1}) between 15° and 32°N with a maximum of 15 mm month^{-1} near 27° N. Tropical cyclones at 27° N contribute nearly 10% to the total rainfall and the maximum is approximately 20° north of the maximum non-tropical cyclone rainfall (Fig. 3b) found in the ITCZ. In the eastern North Atlantic (Fig. 3c), the zone of maximum tropical cyclone

rainfall is nearly half of that found in the western North Atlantic (i.e., 7 mm month^{-1}), occupies a smaller zonal region, contributes less than 4% to the total rainfall, and is located near 11° N. This axis of maximum rainfall is only 5°poleward of the zone of maximum non-tropical cyclone rainfall (Fig. 3d). This North Atlantic zonal analyses indicates that during the tropical cyclone months the western North Atlantic tropical cyclones are more numerous and intense and move to higher latitudes as they begin to interact with the westerlies.

b Seasonal variation of tropical cyclone rainfall

The seasonal variation of the North Atlantic tropical cyclone mean rainfall for the months of June-November is seen in Fig. 4. The figure shows that eastern North Atlantic tropical cyclone rainfall increases from June to September and then decreases after September. The eastern North Atlantic tropical cyclones that contribute rainfall during August and September usually develop from African easterly wave disturbances. They can be the most intense tropical cyclones of the season as they propagate westward towards the North and Central America or recurve northwestward into the westerlies.

In the western North Atlantic, tropical cyclone rainfall can be found throughout the season, with the greatest amounts located in the subtropical regions east-northeast of Puerto Rico during July through September. During June, October, and November, the regions of heavy tropical cyclone rainfall can be found in the Gulf of Mexico or the western Caribbean Sea. These tropical cyclones, however, do not always originate from

the North African easterly wave disturbances, but are sometimes generated in the cyclogenesis regions of the Gulf of Mexico and Caribbean Sea.

Figure 5 shows a histogram of the western (Fig. 5a) and eastern (Fig. 5b) North Atlantic non-tropical cyclone (black bars) and tropical cyclone (dashed bars) monthly mean rainfall amounts. The mean monthly rainfall and the percentage (the percentage is the number above the bar graph) of rainfall contributed by tropical cyclones peaks in August - October in the western North Atlantic, while the tropical cyclone rainfall peaks in September in the eastern North Atlantic. In the western North Atlantic, the months that contain the largest tropical cyclone rainfall amounts (i.e., August through October) coincide with the months that have the greatest non-tropical cyclone rainfall. These tropical cyclones are usually generated by the North Africa easterly wave disturbances, but can also be generated by other atmospheric conditions. However, in the eastern North Atlantic the month with the greatest tropical cyclone rainfall amounts (i.e., September) precede the month with the greatest non-tropical cyclone rainfall. These results suggest that the eastern North Atlantic tropical cyclones generated by the North African easterly wave disturbance were more active and wetter in September, while the combination of the ITCZ and baroclinic systems created greater non-tropical cyclone rainfall during the month of October.

Figure 6a, which shows the zonally averaged mean monthly tropical cyclone rainfall in the western North Atlantic during the early and late summer and fall months, reemphasizes the seasonal change. It is clearly seen that heavy tropical cyclone rainfall

(>20 mm month^{-1}) between 16° and 32° N occurs during the late summer. In the eastern North Atlantic Fig. 6b), it is more clearly seen that there is a late summer tropical cyclone rainfall season. During this time, heavy zonally averaged mean tropical cyclone rainfall (>15 mm month^{-1}) occurs between 10° and 17°N latitude. Light tropical cyclone rainfall of less than 7 mm month^{-1} occurs at all latitudes during the other months. In both the western and eastern North Atlantic regions, the tropical cyclones that create the greatest zonally averaged mean rainfall during the late summer are those that are developed from the North African easterly wave disturbances. It is also noted from the figure that there is no latitudinal shift during the season, unlike what was observed in the western North Pacific (Rodgers et al 2000).

c Rainfall and tropical cyclone intensity

The geographical distribution of tropical cyclone rainfall contributed by depressions, storms, and hurricanes is seen in Fig. 7. Not surprisingly, the figure shows that the greatest tropical cyclone rainfall amounts are contributed by the most intense systems. However, in the eastern North Atlantic region the majority of the tropical cyclone rainfall is light (<15 mm month^{-1}) since it is contributed by depressions and storms. This indicates that during this eleven year period, the majority of the tropical cyclones were developing and had not matured. In the western North Atlantic, there are greater regional rainfall amounts. This is particularly true in the region east-northeast of Puerto Rico. Mean monthly tropical cyclone rainfall amounts exceed 25 mm month^{-1}. The preferred path of maximum hurricane rainfall traces eastward north of the Greater

Antilles, and then splits with one path recurving northeastward into the westerlies and another moving towards the Florida coast. The "bulls eye" hurricane rain maximum off the coast of Honduras is associated with Hurricane Mitch. It is also seen that in the western North Atlantic (30°N/60°W by 40°N/50°W) the greater amounts of rainfall are generated at the higher latitudes by tropical cyclones of hurricane intensity.

However, the statistical information seen in Fig. 8 indicates that even though the most intense tropical cyclones contributed the greatest regional mean monthly rainfall, the greatest mean monthly rainfall over the entire North Atlantic is contributed by tropical cyclones of storm stage (i.e., 0.5 (0.8) mm month^{-1} greater than western (eastern) North Atlantic hurricanes). In addition, eastern North Atlantic depressions contribute greater amounts of rainfall than eastern North Atlantic storms (i.e., nearly 0.4 mm month^{-1} greater). The obvious reasons why these tropical cyclones of storm stage contribute greater regional rainfall is that there are greater number of storms and storm observations during this eleven year period (see figure above the bar graph).

The zonally averaged tropical cyclone rainfall as a function of tropical cyclone intensity for the western (Fig. 9a) and the eastern (Fig. 9b) suggests that as tropical cyclones become more intense there is a narrowing of the zonal peak and a poleward shift. The narrowing of the zonal peak of tropical cyclone rainfall can best be seen in western North Atlantic, while the poleward shift in the maximum zonal tropical cyclone rainfall amount is seen throughout the North Atlantic. Similar to North Pacific tropical cyclones (Rodgers et al 2000), the poleward shift appears to indicate how important the

more intense tropical cyclones are in generating rainfall at higher latitudes throughout the North Atlantic.

d *Inter-annual variation of tropical cyclone rainfall*

Within the North Atlantic basin at time scales sampled in this study, the atmospheric forcing mechanisms that have the greatest control on the inter-annual variation of tropical cyclone frequency and intensity are those related to El Niño Southern Oscillation (ENSO) events. The ENSO events appear to explain approximately 50% of the inter-annual variation of western North Atlantic tropical cyclones (Gray, personal communication). According to Gray (1994a), the enhanced central and eastern North Pacific tropical SSTs and ocean evaporation during the El Niño years help to shift the convective region of the ITCZ more eastward, thereby exposing the North Atlantic to stronger westerly outflow and vertical wind shear. This increase of vertical wind shear over the North Atlantic, in turn, causes an enhancement in upper-tropospheric ventilation and less convective development (Reuter and Yau 1986; De Marua and Huber 1998). During the La Niña and neutral years, on the other hand, there is little eastward shift in the convective region of the ITCZ due to the cooler eastern and central North Pacific SSTs and less vertical wind shear over the North Atlantic. These results were substantiated in the studies that examined the long term history of strike probability and damage caused by hurricane landfall in the western North Atlantic (Johnson and Lupo 1999; Bove et al 1998; Pilke and Landsea 1999). These studies suggested that there is a

greater hurricane strike probability and damage from hurricanes occurring during the La Niña and neutral years than during the El Niño years.

However, as mentioned earlier the inter-annual variation of hurricanes is only partially explained by ENSO events. There are other factors that suppress or enhance the inter-annual variability of the frequency and intensity of North Atlantic tropical cyclones. Other inter-annual varying factors such as the variation of SSTs and surface pressures that these tropical systems encounter and the phase of the Quasi-Biennial Oscillation (Gray 1984 a,b) can influence the frequency and intensity of tropical cyclones. Short term climate changes such as the variation of rainfall in the western Sahel region of Northern Africa (Landsea and Gray 1992) as well as longer term climate changes caused by the linkage between the ocean and atmosphere that is associated with the North Pacific Oscillation (Gershanov and Barnett 1998) and the North Atlantic Oscillation (Hurrell 1995; Gray 1998) may have a longer term effect on the frequency and intensity of tropical cyclones. Therefore, it appears that ENSO events alone do not necessarily produce an anomaly in the frequency and intensity of North Atlantic tropical cyclones, particularly if the ENSO event is weak.

Tropical cyclone rainfall anomalies for each individual year are seen in Fig. 10. The rainfall anomalies are constructed by subtracting the mean July-November climatological tropical cyclone rainfall from the mean July-November tropical cyclone rainfall for each of the eleven years. It is seen that unlike the North Pacific (Rodgers et al 2000), the inter-annual variation in the North Atlantic tropical cyclone rainfall during most of the tropical cyclone years is smaller due to the less frequent and weaker sampled

North Atlantic tropical cyclones (i.e., compare Table 1 of Rodgers et al. 2000 with Table 1 of this paper). It is noted in Figs. 10 and 11 that during 1995 and 1996 there is greater than average tropical cyclone rainfall north of the Greater Antilles and over the entire domain of the western North Atlantic as shown by the histograms and percentages.

The time history of the Niño 3.4 (i.e., 5°–5°S and 120°-170°W) SSTs seen in Fig. 12, indicates that during July-November months of this eleven year period there were three El Niño/La Niña events that clearly showed warm SST anomalies followed by cool SST anomalies (1987/1988, 1994/1995, and 1997/1998) (Barston and Ropelewski 1992). These two year couplets are delineated in Fig. 11 as an E for the El Niño year and a L for the La Niña year. The three couplet years show clear evidence of an ENSO signal in the pattern (Fig. 10) and statistics (Fig. 11) of the tropical cyclone rainfall that would be expected in the North Atlantic. It is clear from Figs. 10 and 11 that the years with limited amount of tropical cyclonic rainfall during the El Niño years are followed by a year with above normal tropical cyclone rainfall during the La Niña years. The La Niña effect in 1995 continues into 1996 with negative SST anomalies in the Pacific (Fig. 12) and large amounts and percentages of tropical cyclone rainfall in the Atlantic.

To further verify that Niño 3.4 SSTs have a greater effect on the inter-annual variation of the North Atlantic tropical cyclone rainfall than the regional North Atlantic SSTs, a plan view of the difference between North Atlantic SSTs during the three couplet ENSO events of 1987/1988, 1994/1995, and 1997/1998 are shown in Fig. 13. The figure clearly demonstrates that the North Atlantic SSTs differences are not consistent during

these ENSO events as compared to those in the eastern and central North Pacific (Rodgers et al. (2000) and, therefore, appears to have less affect on the inter annual variation of North Atlantic tropical cyclone rainfall. Unlike the North Pacific tropical cyclone rainfall study (Rodgers, et. al. 2000), the North Atlantic tropical cyclone rainfall patterns (Fig. 10) and statistics (Fig. 11) during the years of 1991-1993 appear to have a greater relationship to the ENSO induced Niño 3.4 SST anomalies. The histogram and percentages indicated that tropical cyclone rainfall was reduced during this time period.

To examine further the relationship between tropical cyclone rainfall and the Ninõ 3.4 SST anomalies for the tropical cyclone season during the eleven year period, a linear regression is performed. The linear regression line and the correlation coefficient between the Ninõ 3.4 SST anomalies and western and eastern North Atlantic tropical cyclone rainfall are seen in Fig. 14. The figure clearly shows a negative correlation coefficient between the parameters of -.52 and -.67 respectively, in the western and eastern North Atlantic, while the correlation coefficient between Ninõ 3.4 SST anomalies and non-tropical cyclone rainfall for both the western and eastern North Atlantic is nearly zero (figure not shown)..

The difference between the El Niño/La Niña pattern for the non-tropical cyclone and tropical cyclone rainfall across the western and eastern North Atlantic is seen in Fig. 15. The figures are constructed by taking the differences between El Niño years and the La Niña years of the three couplet years. The upper panel of the figure indicates that there is a small decrease (> -80 mm month^{-1}) in the mean rainfall contributed by North

Atlantic non-tropical cyclone systems along the ITCZ (i.e., from 30° W to Central America). On the other hand, there is a small increase in rainfall (< 80 mm month^{-1}) within the subtropical regions of the North Atlantic east of North America and between 30°- 50° W during the El Niño years.

The lower panel of Fig. 15 (scale is smaller than upper panel) shows that tropical cyclone rainfall is less (> -35 mm month^{-1}) over the majority of the North Atlantic during the El Niño years than during the La Niña years. The only exception is within a limited area of the North Atlantic subtropics north of the Lesser Antilles where mean tropical cyclone rainfall was greater (< 15 mm month^{-1}) during El Niño years . It is interesting to note, but not surprising, that the enhanced vertical wind shear that is more prevalent during the El Niño years appears to influence not only the convection in the tropical cyclones, but convection within the ITCZ of the North Atlantic .

The zonally averaged non-tropical cyclone and tropical cyclone mean monthly rainfall during the El Niño/La Niña years is shown in Fig. 16 for the western and eastern North Atlantic. The figure indicates that there is little difference in the zonally averaged non-tropical cyclone rainfall between the El Niño and La Niña periods for both the western (Fig. 16b) and eastern (16d) North Atlantic. Not surprising, the zonally averaged tropical cyclone rainfall during the El Niño years was less than those during the La Niña periods for both the western (Fig. 16a) and eastern (16c) North Atlantic. This was particularly true in the tropical regions (<20° N) of the western North Atlantic and in the subtropical area (>20°N) of the eastern North Atlantic.

Table 1. The total number of tropical cyclones and tropical cyclones of depression, storm, and moderate (Vmax 32-64 ms^{-1}) and strong (Vmax >64 ms^{-1}) hurricane intensity observed from all available SSM/Is in the western and central North Atlantic during July-November of the three El Niño and La Niña years.

North Atlantic El Niño/La Niña Years		
	Western	**Eastern**
Depressions	**10/14**	**6/11**
Storms	**11/20**	**9/20**
Moderate Hurricanes	**6/14**	**2/13**
Strong Hurricanes	**0/1**	**0/0**
All Tropical Cyclones	**27/49**	**17/44**

The North Atlantic tropical cyclone frequency and intensity data for the three El Niño/La Niña couplet years are seen in Table 1. The table reveals that there are also differences in the number and intensity of the North Atlantic tropical cyclones during the warm and cool ENSO events. The information in the table clearly demonstrates that the total number of western and eastern North Atlantic tropical cyclones are considerably

greater during the La Niña years as compared to those during the El Niño years. It is also observed that there are more intense western and eastern North Atlantic tropical cyclones during the La Niña years. These statistical findings are not surprising and support the tropical cyclone rainfall information previously mentioned.

4 Conclusions and Summary

Similar to the North Pacific tropical cyclone study (Rodgers et al. 2000), rainfall estimates made from satellite passive microwave (SSM/I) observations are used to estimate the North Atlantic monthly rainfall amounts contributed by tropical cyclones that became storm intensity and greater. These rainfall estimates during the approximate years of 1987-1998 were used to assess the impact of tropical cyclone rainfall on the geographical, seasonal, and intra-annual distribution of total rainfall.

The main results of this study suggest the following.

1) Tropical cyclones contribute, respectively, 4%, 3%,and 4% to the total western, eastern, and the entire North Atlantic rainfall during the tropical cyclone season. The greatest contributions of rainfall from tropical cyclones is nearly 30% and are found northeast of Puerto Rico, within the middle subtropical North Atlantic, and west of Africa. Much like the North Pacific, it appears that tropical cyclones can augment the rainfall during the North Atlantic growing season, particularly near the lesser and greater Antilles Islands, Mexico, Central America, and the

southeastern United States and can be a significant source of water for agriculture and other purposes.

2) The maximum zonally averaged tropical cyclone rainfall is located poleward of the maximum zonally averaged non-tropical cyclone rainfall within the North Atlantic. This is particularly true in the western North Atlantic where tropical cyclones recurve northwards under the influence of the westerlies.

3) The greatest amount of tropical cyclone rainfall is contributed by systems of storm intensity in both the western and eastern North Atlantic due to the greater frequency. However, there is a greater frequency of tropical cyclones at all intensities in the western North Atlantic and, therefore, more tropical cyclone generated rainfall.

4) There is no monthly lag between maximum tropical cyclone rainfall and maximum non-tropical cyclone rainfall in the western North Atlantic, while in the eastern North Atlantic maximum tropical cyclone rainfall precedes maximum non-tropical cyclone rainfall. This lag may be attributed to the fact that tropical cyclone rainfall is more dependent on the frequency of African easterly wave disturbances that reach their maximum in late August and early September, while non-tropical cyclone rainfall is mostly dependent on the presence and strength of both the ITCZ and baroclinic systems that reach their combined maximum in October.

5) Unlike the North Pacific tropical cyclone climatology rainfall study, the warm ENSO events have a opposite affect on the tropical cyclone rainfall over the North Atlantic by inhibiting tropical cyclone rainfall by subjecting these systems to greater upper-tropospheric ventilation and vertical wind shear. At the same time, warm or cool ENSO years had little influence on the non-tropical cyclone rainfall. Also unlike the North Pacific tropical cyclone rainfall climatology study, the tropical cyclone rainfall differences during the couplet El Niño/La Niña years of 1987/1988, 1994/1995 and 1997/1998 were much less in the North Atlantic basin than that found in the North Pacific, due to weaker and less frequent numbers of tropical cyclones

6) Finally, the satellite estimated tropical cyclone rainfall observations during the couplet El Niño/La Niña years of 1987/1988, 1994/1995 and 1997/1998 were consistent with the early North Atlantic tropical cyclone studies in that the amount of tropical cyclone rainfall was influenced more by atmospheric forcing than by sea surface energy flux processes.

Acknowledgements: Funding support was provided by NASA Office of Earth Science. The authors would like to thank Dr. Ramesh Kakar of NASA Headquarters for his support of this work.

REFERENCES

Adler, R. F., H.-Y. M. Yea, N. Prasad, W-K. Tao, and J. Simpson, 1991: Microwave simulations of a tropical rainfall system with a three-dimensional cloud model. *J. Appl. Meteor.*, **30**, 924-953.

Adler, R. F., G. J. Huffman, and P. R. Keehn, 1994: Global tropical rain estimates from microwave-adjusted geosynchronous IR data. *Remote Sensing Reviews.* **11**, 125-152.

Barnston, A. G., and C. F. Ropelewski, 1992: Prediction of ENSO episodes using canonical correlation analysis. *J. Climate*, **7**, 1316-1345.

Bell, T. L., P. K. Kunda, and C. Kummerow, 1996: Sampling errors of satellite estimates of gridded rainfall. Preprints. *13th Conf. on Probability and Statistics in the Atmospheric Science.* San Francisco, Calif. Amer. Meteor. Soc., 298-

Bove, M.C.,J. B.Elsner, C.W.Landsea ,N. Xufeng.and J. .J. O'Brian Effect of El Niño on landfall hurricanes. Bul. Amer Meteor . Soc.,**79**, 2477-2482.

De Maria, M. and M. M. Huber, 1998: The effects of vertical shear on tropical cyclone intensity change. An historical perspective. *Preprints, Symposium on Tropical Cyclone Intensity Change. Amer. Meteor. Soc.*, pp 22-29.

Gershanov, A. and T. P. Barnett, 1998: Inderdecadal modulation of ENSO teleconnections. *Bul. Amer. Meteor. Soc.*, **79**, 2715-2725.

Gray W. M. 1984a: Atlantic seasonal hurricane frequency . Part 1. El Niño and 30 mb qiasi-biennial oscillation influence. *Mon. Wea. Rev.*, **112**, 1649-1668.

Gray W. M. 1984a: Atlantic seasonal hurricane frequency. Part II. Forecasting its variability. *Mon. Wea. Rev.*, **112**, 1669-1683.

Gray, W. M., 1998: Hypothesis on the cause of global multidecadal climate change. *Preprints of the Ninth Symposium on Global Change Studies*, Dallas, Tx, Amer. Meteor. Soc., 271-275.

Hollinger, J, T., 1991: DMSP Special Sensor Microwave/Imager calibration/validation final report. Vol. 11. Naval Research Laboratory, 12-25 pp.

Hurell, J. W., 1995: Decadal trends in the North Atlantic Oscillation. Regional temperature and precipitation. Science, 269, 676-679.

Johnson, G., and A. R. Lupo, 1999: The interannual variability of Atlantic basin hurricane activity. *8th Conf. On Climate Variation,* Denver, Co.., Amer. Meteor. Soc. , 118-121.

Landsea, C. W. and W. M. Gray, 1992: The strong association between western Sahel monsoon rainfall and intense Atlantic hurricanes. *J. Climate*, **5**, 435-453.

Pilke, R. A. Jr. and C. N. Landsea, 1999: La Niña, El Niño and Atlantic hurricane damages to the United States. *Bull. Amer. Soc.*, **80**, 2027-2034.

Reynolds, R. W. and T. S. Smith, 1994: Improved global sea surface temperature analyses. *J. Climate,* **5**. 929-948.

Rodgers, E. B., S. W. Chang, and H. F. Pierce, 1994: A satellite-observational and numerical study of precipitation characteristics in western North Atlantic tropical cyclones. *J. Appl. Meteor.*, **33**, 129-139.

Rodgers, E. B., R. F. Adler, and H. F. Pierce, 2000: Contribution of tropical cyclones to the North Pacific climatological rainfall as observed from Satellite. *Jou. Of Appl. Meteor.*, (to be published).

Rueter, G. W., and M. K. Yau, 1986: Numerical modeling of cloud development in a sheared environment. *Bettr. Phys. Atmosph.*, **60**, 65-80.-

TABLE

Table 1. The total number of tropical cyclones and tropical cyclones of depression, storm, and moderate (Vmax 32-64 ms^{-1}) and strong (Vmax >64 ms^{-1}) hurricane intensity observed from all available SSM/Is in the western and central North Atlantic during July-November of the three El Niño and La Niña years.

FIGURES

Fig. 1 Plan view of the North Atlantic showing the designated western and eastern regions (within boxes) that were sampled for total, non-tropical cyclone, and tropical cyclone mean monthly rainfall.

Fig 2 A plan view showing the SSM/I-derived mean monthly North Atlantic rainfall amounts (mm $month^{-1}$) contributed by non-tropical cyclone systems (upper panel) and tropical cyclones (middle panel), and the fractional amount of tropical cyclone rainfall (percentage) (lower panel) for the months of July-November 1987, June-November 1988-1989, and 1991-1998 (65 month period). Brown and blue background

designate, respectively, non-raining land and oceans. The color bar code delineates the percentage and rainfall amounts above each figure.

Fig. 3 The SSM/I-derived 2.5° latitudinal non-tropical cyclone and tropical cyclone zonally averaged mean monthly rainfall amounts (mm month^{-1}) for, respectively, the (a and b) western and (c and d) eastern North Atlantic for the 65 month period.

Fig. 4 A plan view showing the SSM/I-derived mean monthly North Atlantic tropical cyclone rainfall amounts (mm month^{-1}) contributed by tropical cyclones for 1988, 1989, and 1991-1998 for the months of June-November. The white background designate non-raining land and oceans areas. The gray bar code delineates the rainfall amounts.

Fig. 5 A histogram showing the SSM/I-derived averaged mean monthly rainfall amounts (mm month^{-1}) contributed by non-tropical cyclones systems (dark shade) and tropical cyclones (hatched shade) for 1988, 1989, and 1991-1998 during June-November for the (a) western and (b) eastern North Atlantic. Percentage above the bar graph represents the percentage of rainfall contributed by tropical cyclones during the month.

Fig. 6 The SSM/I-derived 2.5° latitude zonally averaged mean monthly rainfall amounts (mm month^{-1}) contributed by tropical cyclones for 1988, 1989, and 1991-1998

during the early summer (June-July), late summer (August-September), and fall (October-November) seasons for the (a) western and (b) eastern North Atlantic.

Fig. 7 A plan view showing the SSM/I-derived mean monthly North Atlantic tropical cyclone rainfall amounts (mm month^{-1}) contributed by tropical cyclones at depression, storm, and hurricane stage during June-November of 1988, 1989, and 1991-1998. The white background designate non-raining land and oceans areas. The gray bar code delineates the rainfall amounts.

Fig. 8 A histogram showing the SSM/I-derived mean monthly rainfall amounts (mm month^{-1}), percentage of contribution, and number of observations for the western (dark shade) and eastern (light hatched) North Atlantic tropical cyclones at depression, storm, and hurricane stage during the 65 month period.

Fig. 9 The SSM/I-derived 2.5° latitudinal zonally averaged mean monthly rainfall amounts (mm month^{-1}) contributed by the (a) western and (b) eastern North Atlantic tropical cyclones of depression, storm, and hurricane stage during the 65 months period.

Fig. 10 A plan view showing the SSM/I-derived mean monthly North Atlantic tropical cyclone rainfall anomalies (mm month^{-1}) for the years of 1987-1989 and 1991-1998 during July-November period. White background designate non-raining land and

oceans areas. The light and dark shades delineates, respectively, the positive and negative rainfall anomalies.

Fig. 11 A histogram showing the SSM/I-derived non-tropical cyclone (dark shade) and tropical cyclone (hatched shade) mean monthly rainfall amounts (mm month^{-1}) for the (a) western and (b) eastern North Atlantic during the July-November period for the years of 1987-1989 and 1991-1998. Percentage values indicate the fractional amount of rainfall contributed by tropical cyclones. "Es" and "Ls" represent, El Niño and La Niña years as defined by the Niño 3.4 SST anomalies.

Fig. 12 Time history of the SST anomalies (°C) in the Niño 3.4 region from 1980-1999. Light (dark) shades represent positive (negative) SST anomalies.

Fig. 13 A plan view showing the SST differences (°C) between El Niño and La Niña couplet years (1987/1988, 1994/1995, and 1997/1998) over the North Atlantic during the month of September..

Fig. 14 A scatter plot of the tropical eastern North Atlantic SST anomalies in the 3.4 Niño region and the mean monthly rainfall amounts (mm month^{-1}) contributed by tropical cyclones during July-November period for the years of 1987-1989, and 1991-1998 for the (a) western and (b) eastern North Pacific. The best-fit line (broad), the equation of the line, and the linear correlation coefficient are shown for each North Atlantic ocean basin.

Fig. 15 A plan view of the difference between the mean monthly rainfall amounts (mm month^{-1}) contributed by the North Atlantic non-tropical cyclone systems (top panel) and tropical cyclones (bottom panel) during El Niño years (1987, 1994, and 1997) minus the La Niña years (1988, 1995, and 1998). Brown and blue background designate, respectively, non-raining land and oceans areas. The color bar code delineates the rainfall differences.

Fig. 16 The SSM/I-derived 2.5° latitudinal zonally averaged mean monthly rainfall amounts (mm month^{-1}) for the tropical cyclones and non-tropical cyclones, respectively, for the (a and b) western and (c and d) eastern North Atlantic during the El Niño (solid lines) and La Niña years (dashed lines).

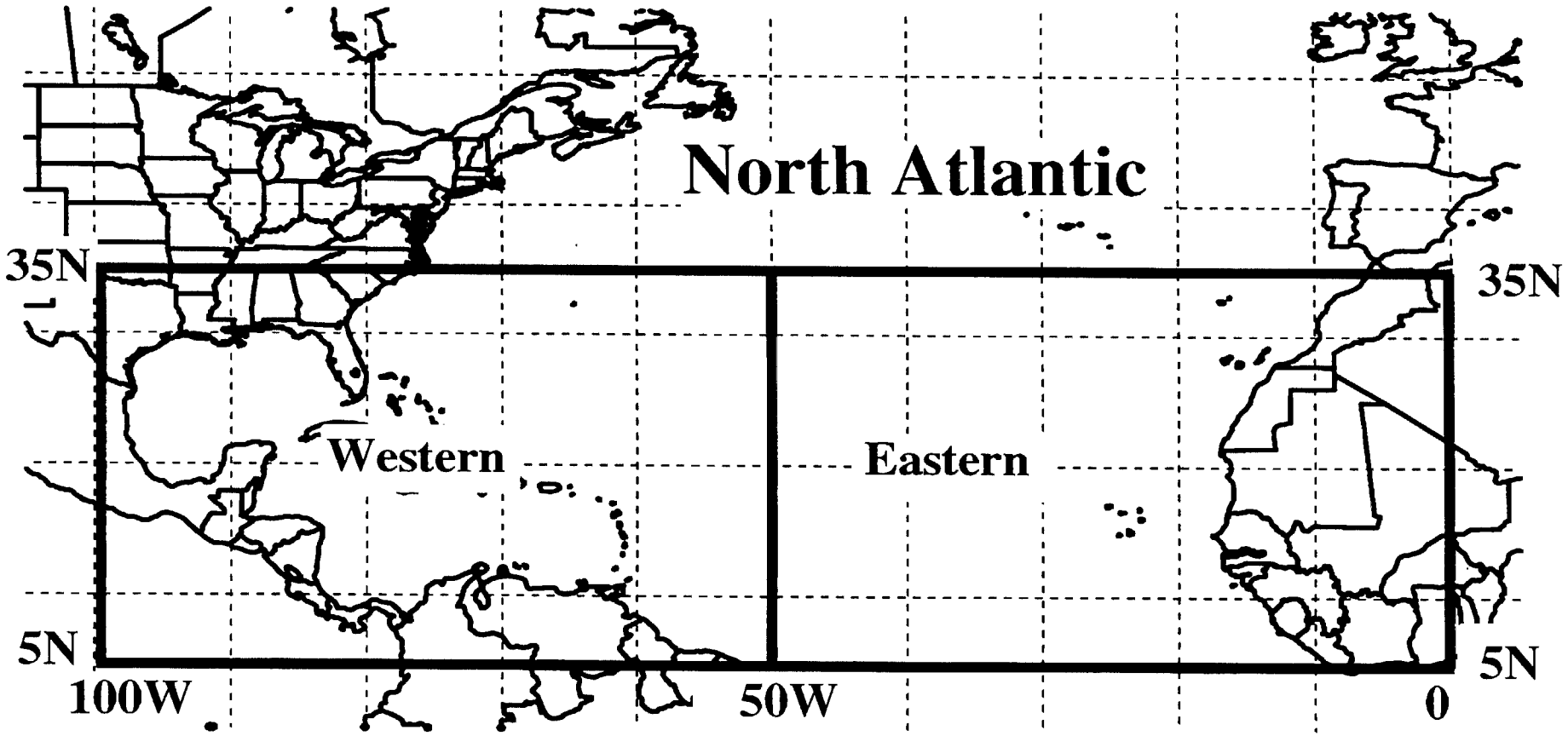

Figure 1

Non–Tropical Cyclone Rain

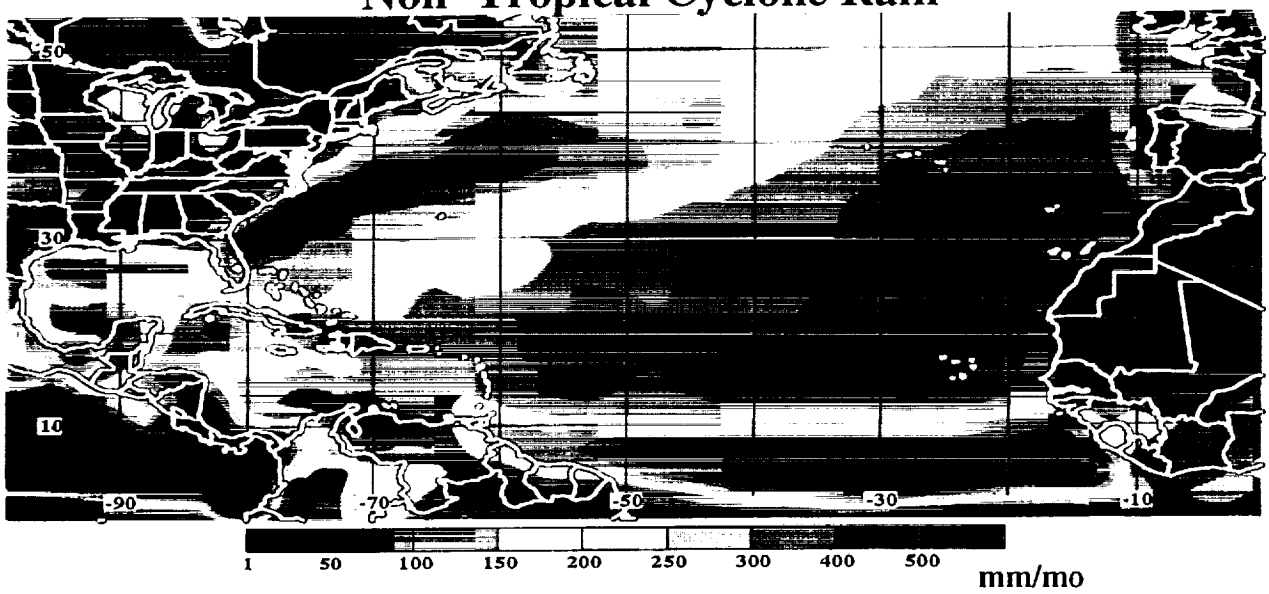

Tropical Cyclone Rain

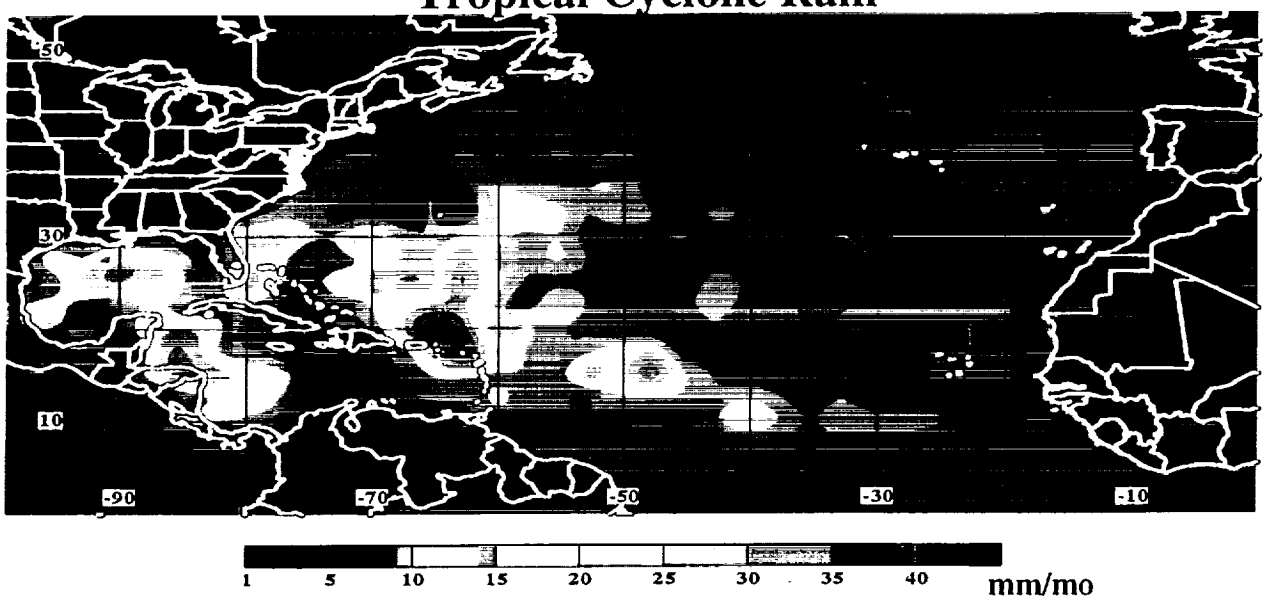

Percentage Tropical Cyclone Rain

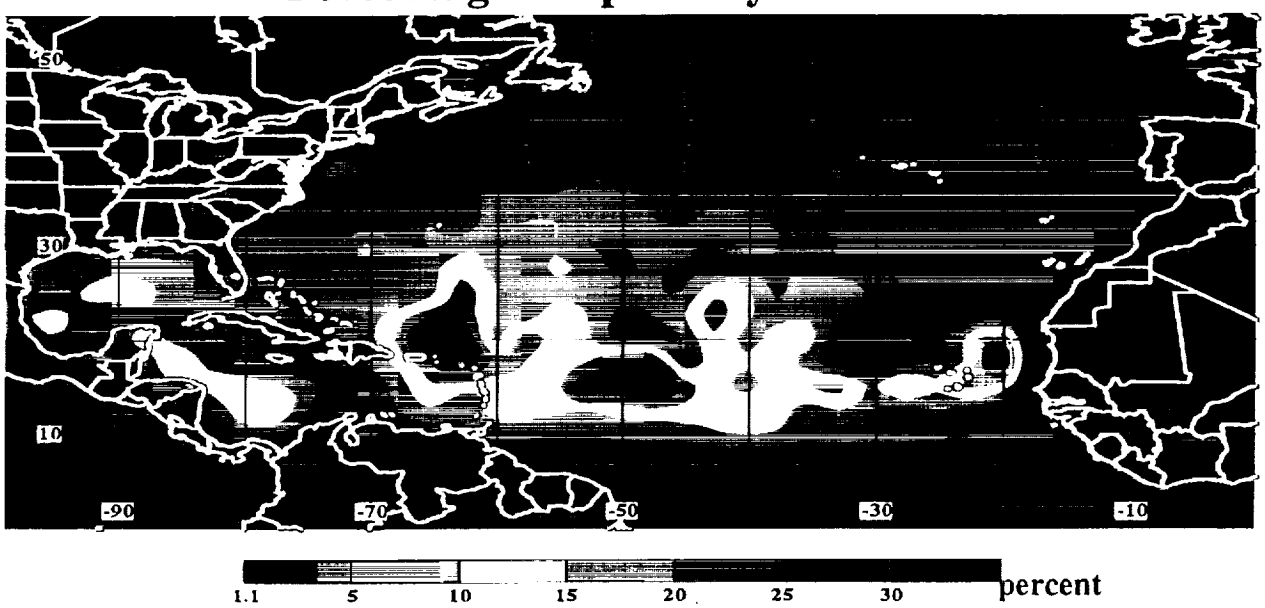

Figure 2

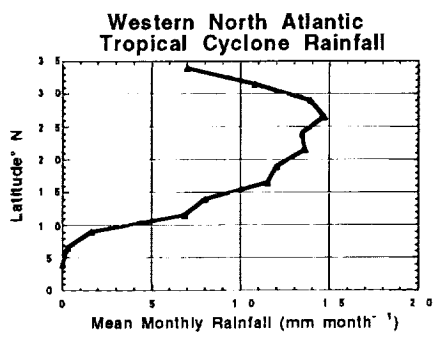

a

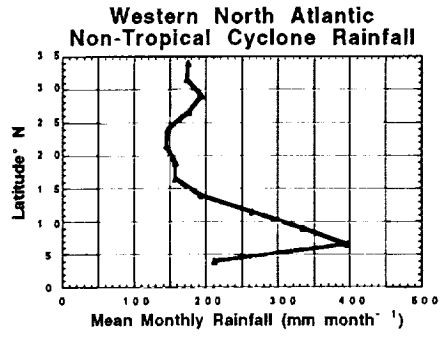

b

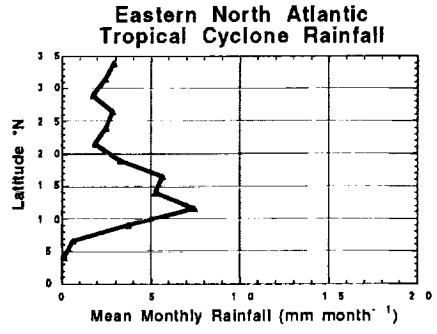

c

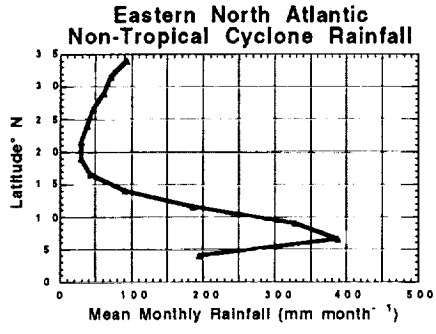

d

Figure 3

Tropical Cyclone Rainrate 1987–1998

June

July

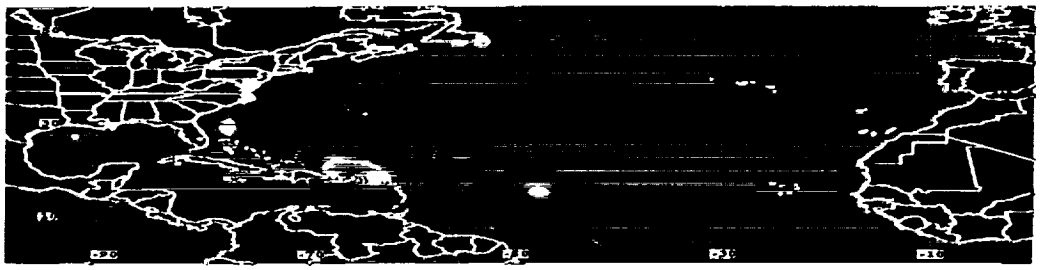

August

September

October

November

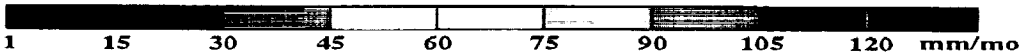

Figure 4

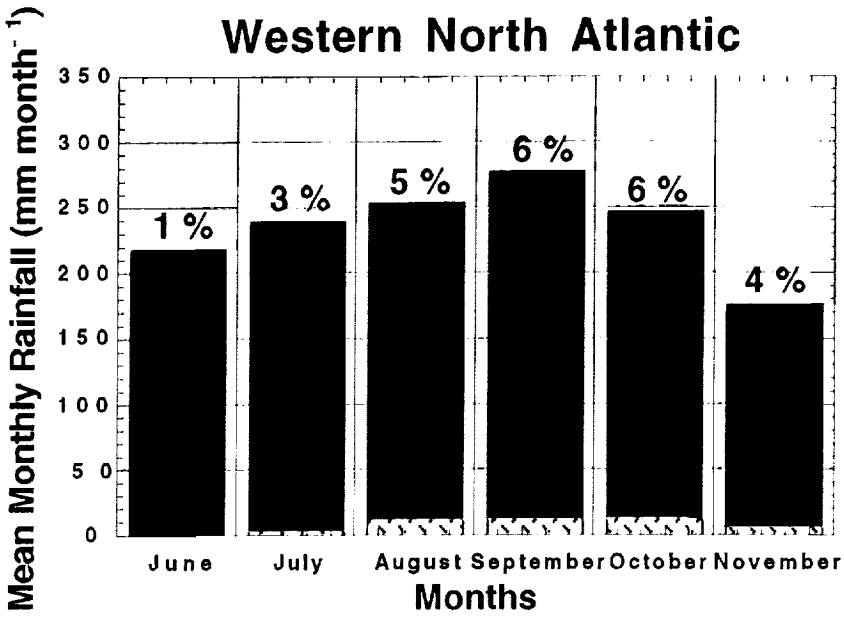
Western North Atlantic
Mean Monthly Rainfall (mm month-1)
350
300
250
200
150
100
50
0
1 %
3 %
5 %
6 %
6 %
4 %
June
July
August
September
October
November
Months

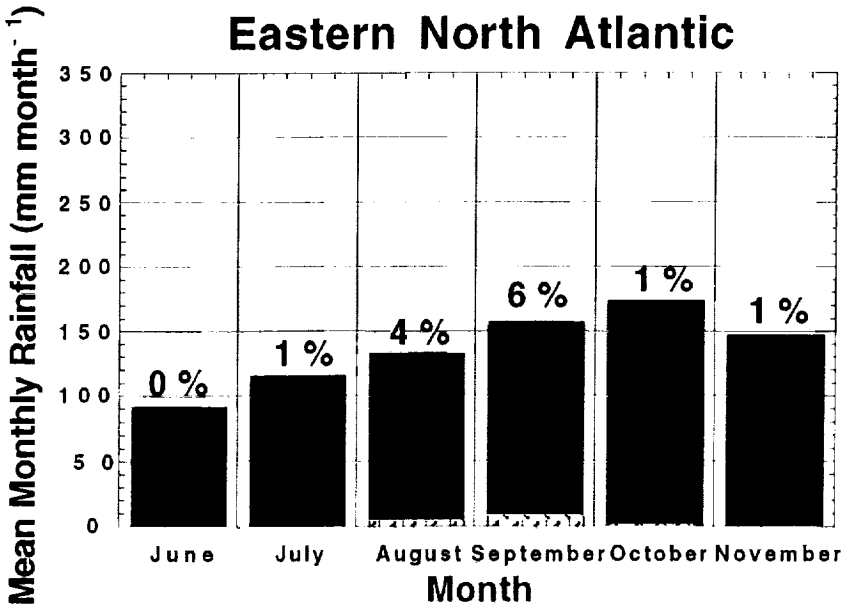
Eastern North Atlantic
Mean Monthly Rainfall (mm month-1)
350
300
250
200
150
100
50
0
0 %
1 %
4 %
6 %
1 %
1 %
June
July
August
September
October
November
Month

Figure 5

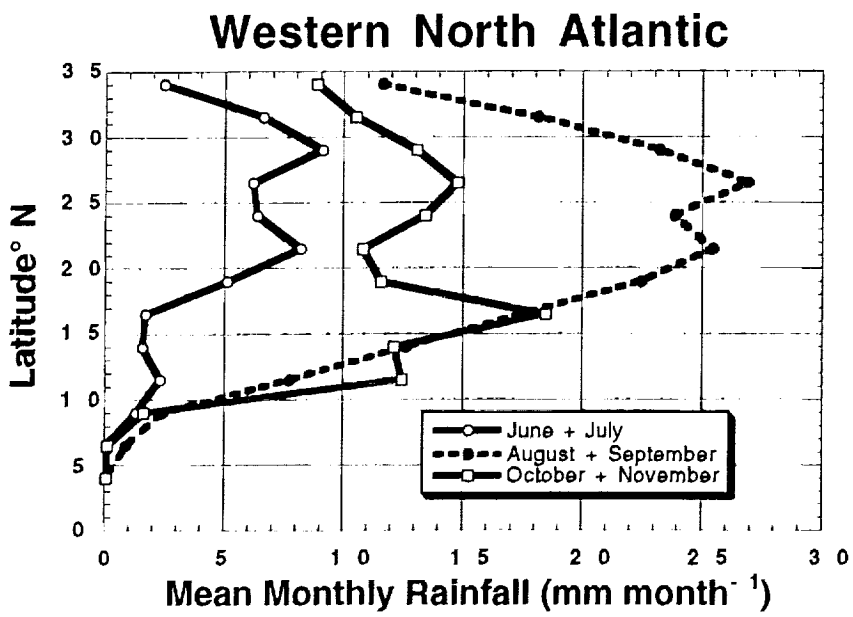
Western North Atlantic
Latitude° N
35
30
25
20
15
10
5
0
0
5
10
15
20
25
30
Mean Monthly Rainfall (mm month⁻¹)
June + July
August + September
October + November

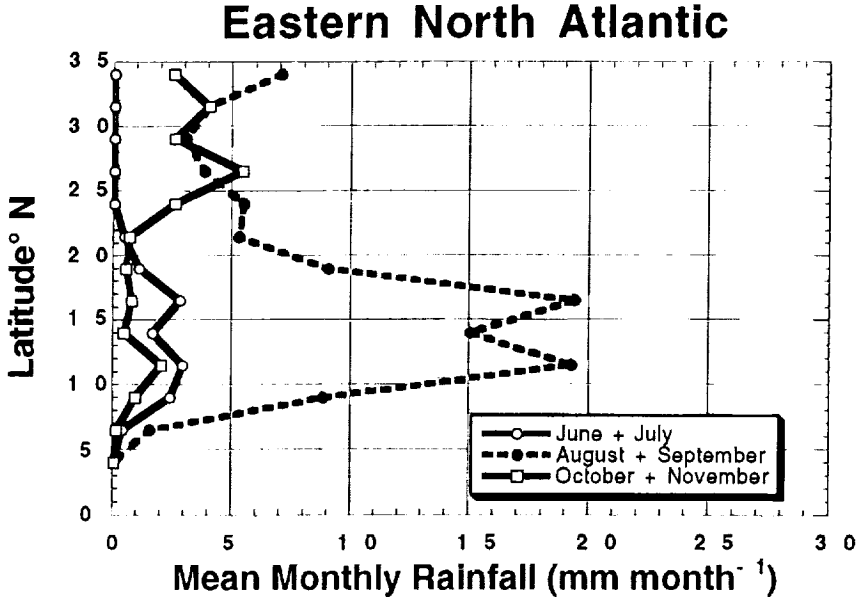
Eastern North Atlantic
Latitude° N
35
30
25
20
15
10
5
0
0
5
10
15
20
25
30
Mean Monthly Rainfall (mm month⁻¹)
June + July
August + September
October + November

Figure 6

1987–1998 Monthly Tropical Cyclone Rainrates

Tropical Depression

Tropical Storm

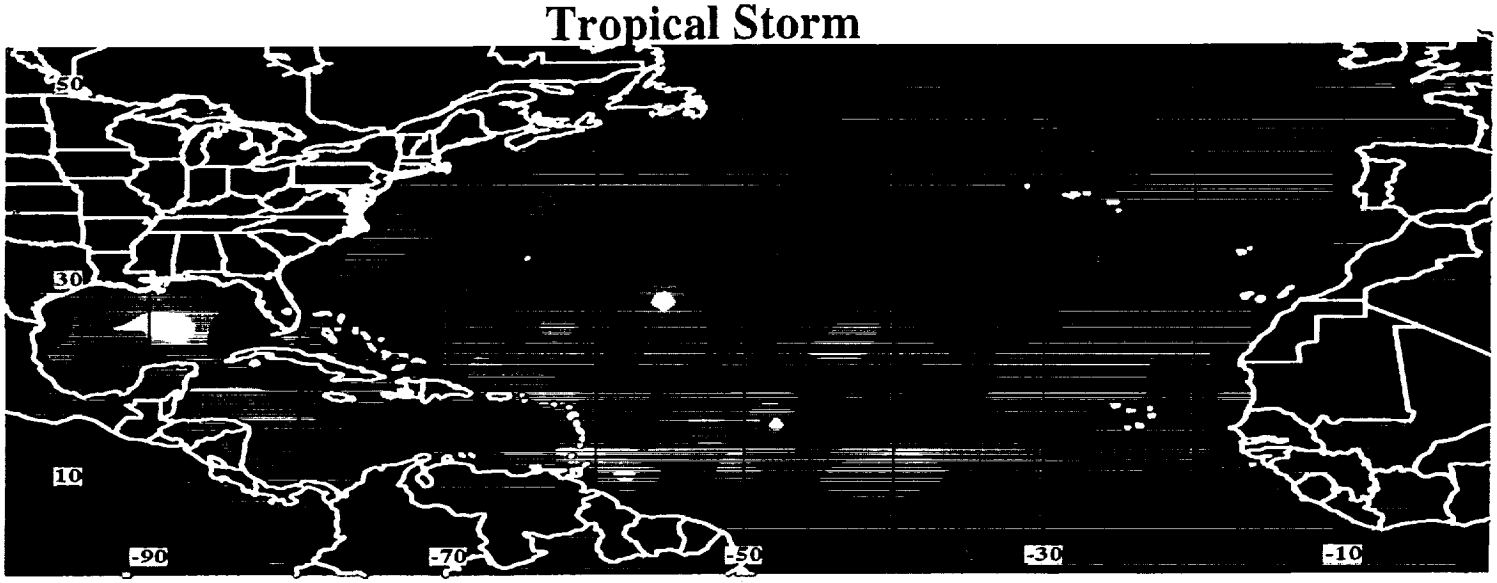

Hurricane

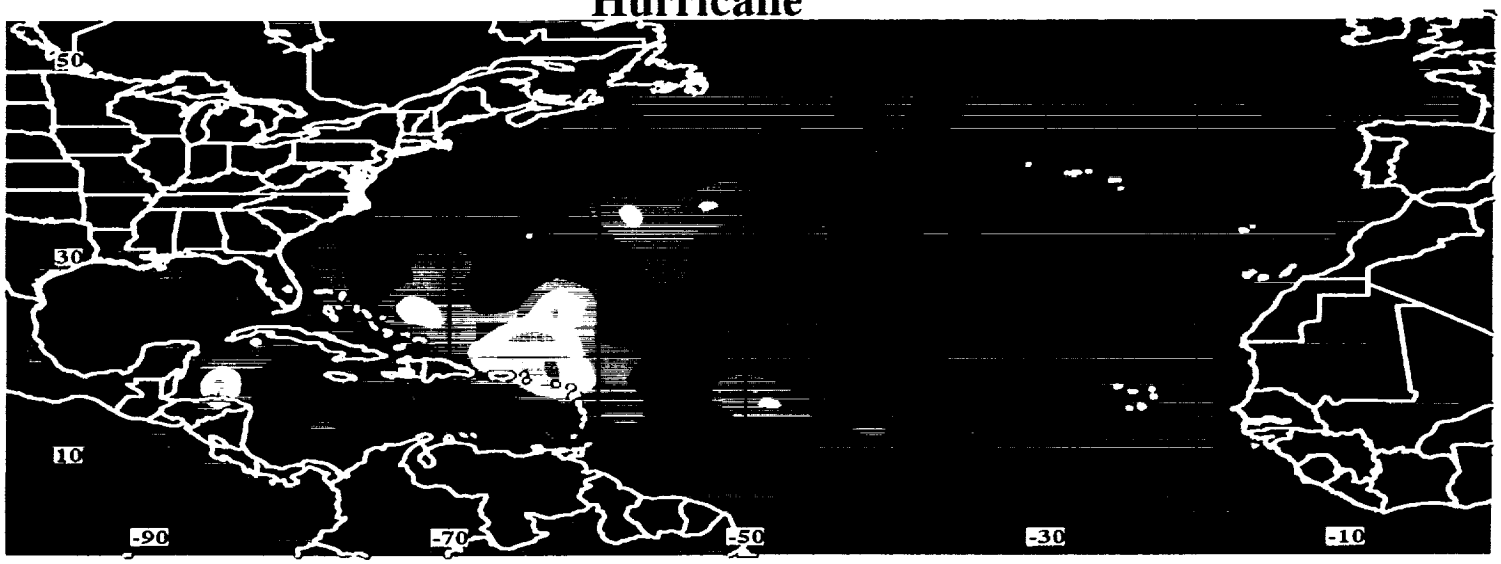

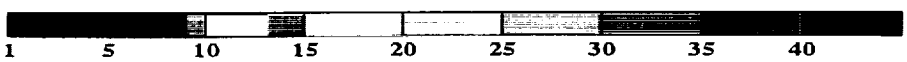

mm/mo

Figure 7

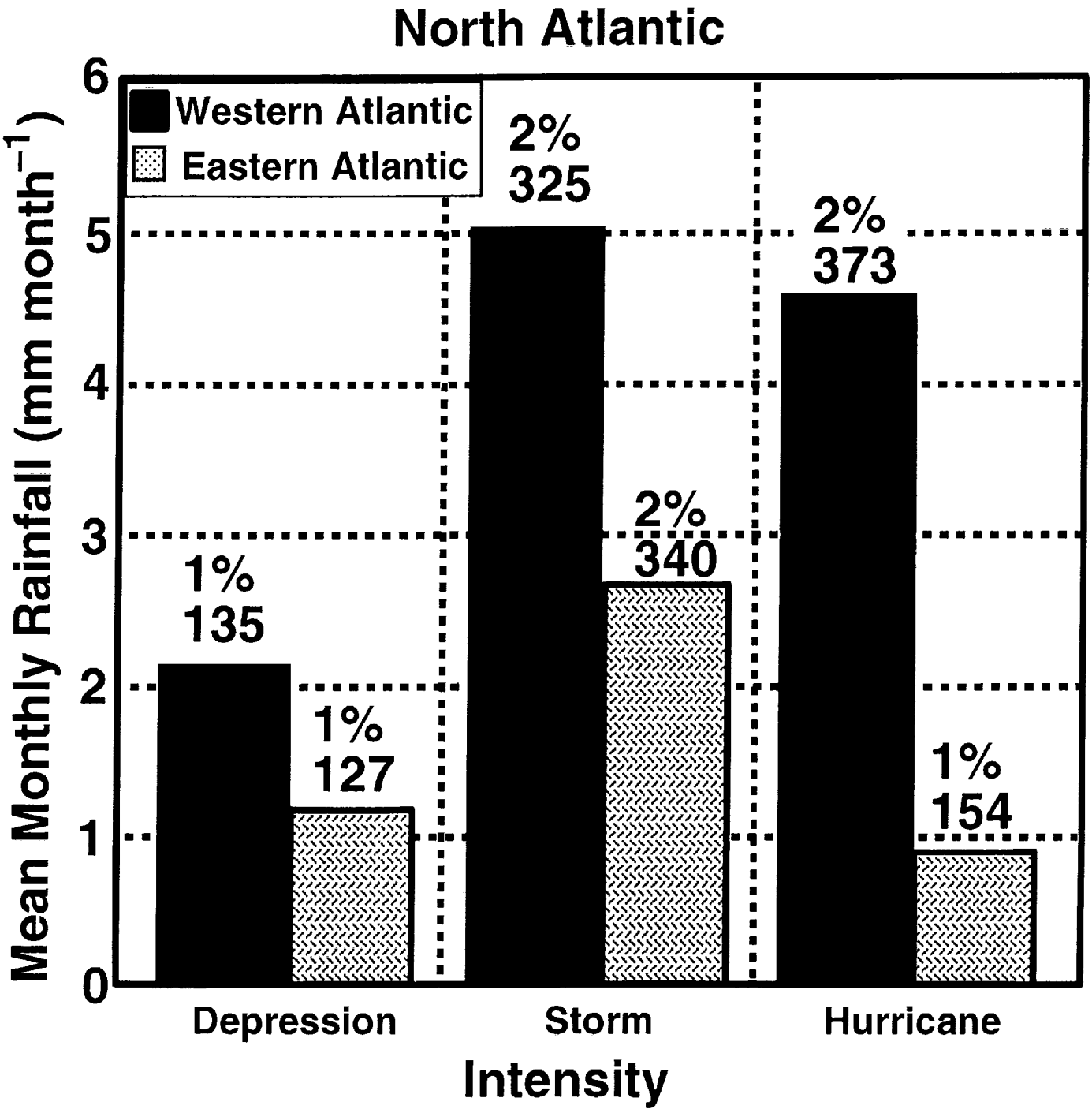
North Atlantic
Western Atlantic
Eastern Atlantic
Mean Monthly Rainfall (mm month^{-1})
6
5
4
3
2
1
0
1%
135
1%
127
2%
325
2%
340
2%
373
1%
154
Depression
Storm
Hurricane
Intensity

Figure 8

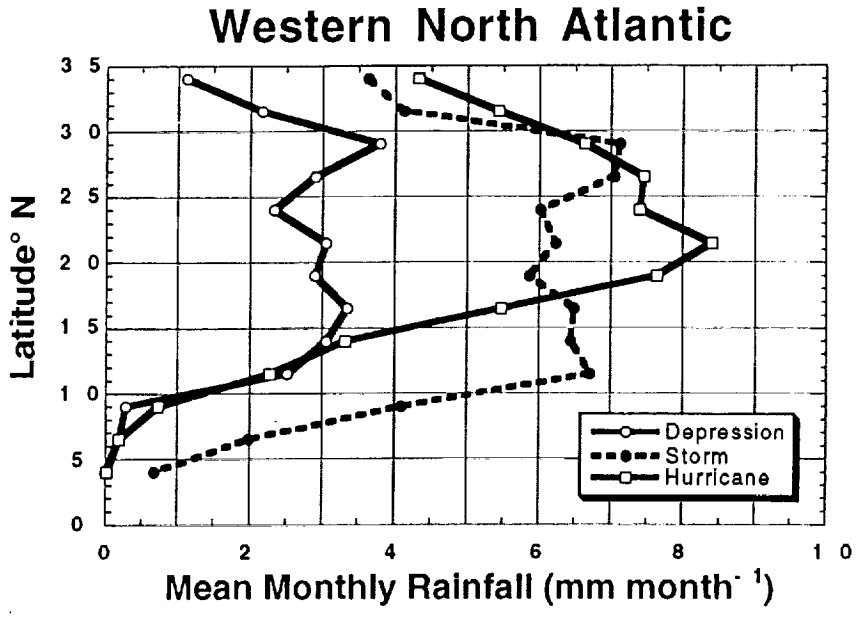
Western North Atlantic
Latitude° N
35
30
25
20
15
10
5
0
0
2
4
6
8
10
Mean Monthly Rainfall (mm month⁻ ¹)
Depression
Storm
Hurricane

a

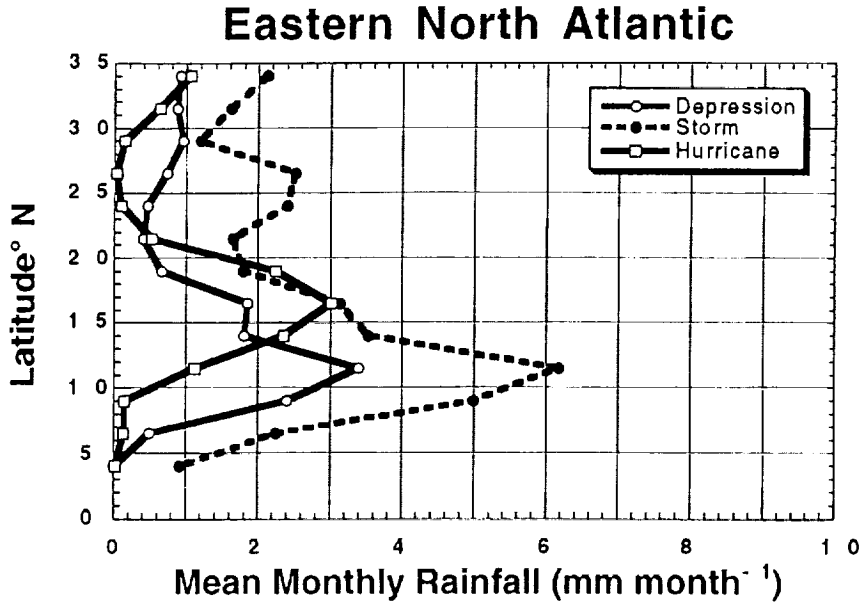
Eastern North Atlantic
Latitude° N
35
30
25
20
15
10
5
0
0
2
4
6
8
10
Mean Monthly Rainfall (mm month⁻ ¹)
Depression
Storm
Hurricane

b

Figure 9

Mean Monthly Tropical Cyclone Rain Anomalies

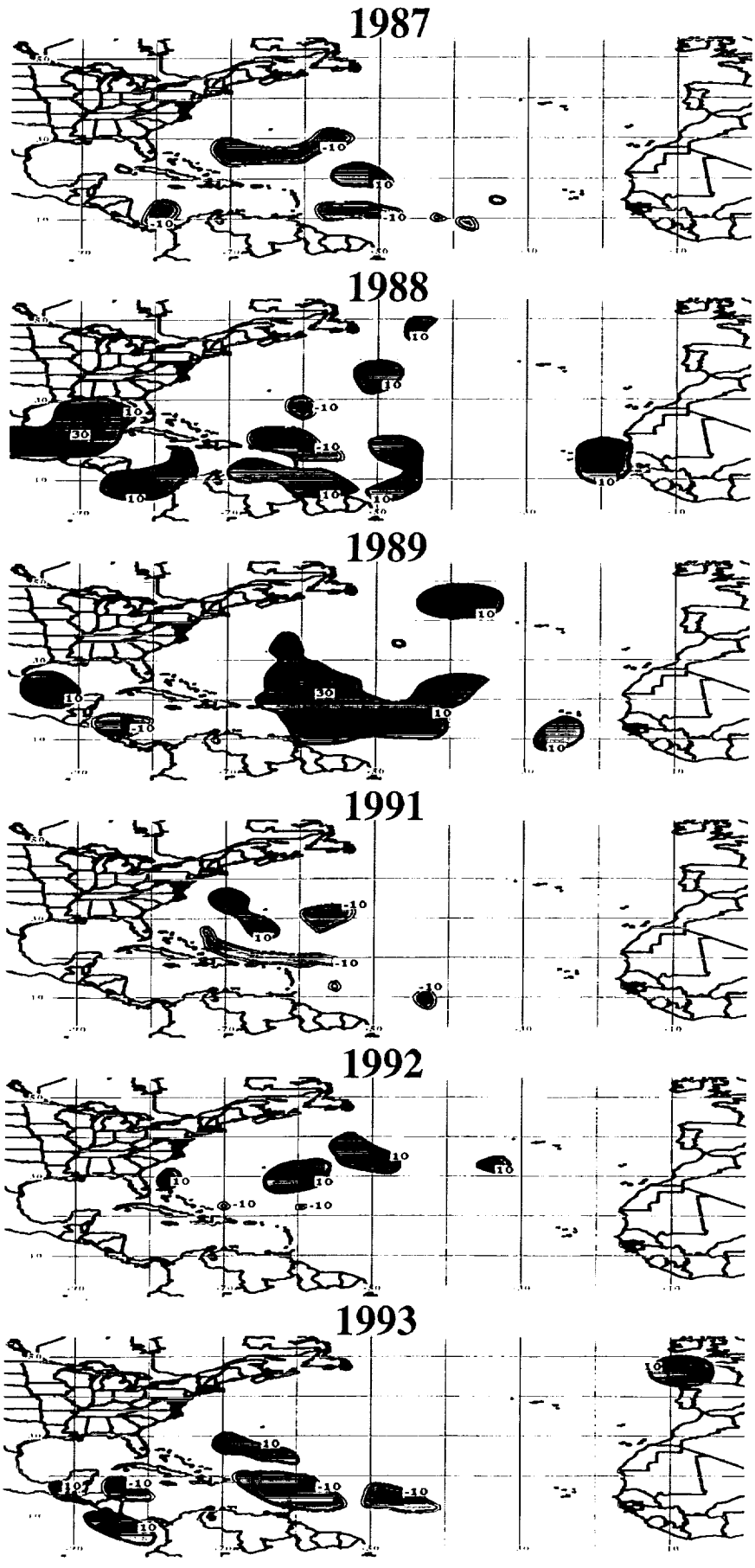

Figure 10a

Mean Monthly Tropical Cyclone Rain Anomalies

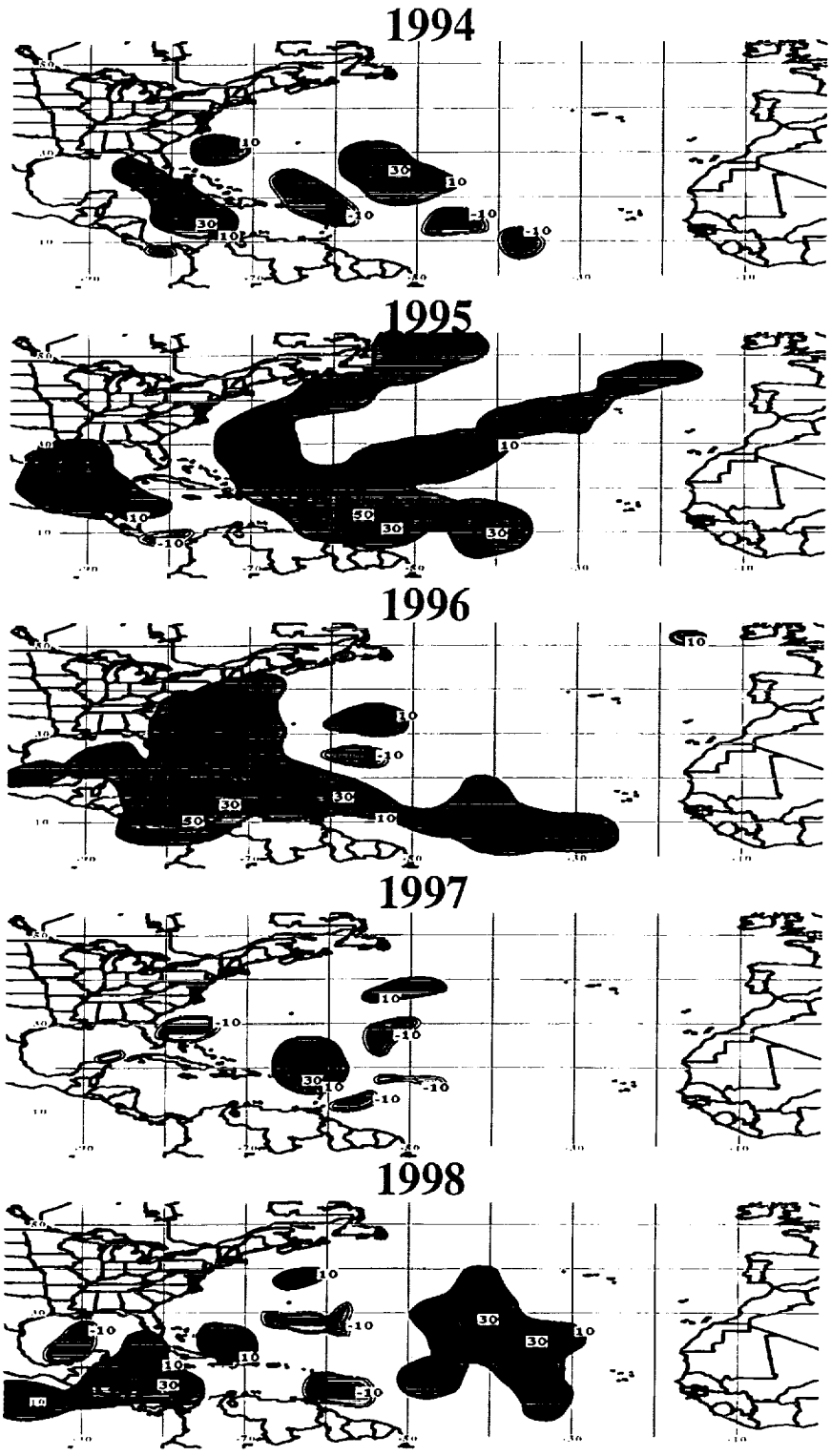

Figure 10b

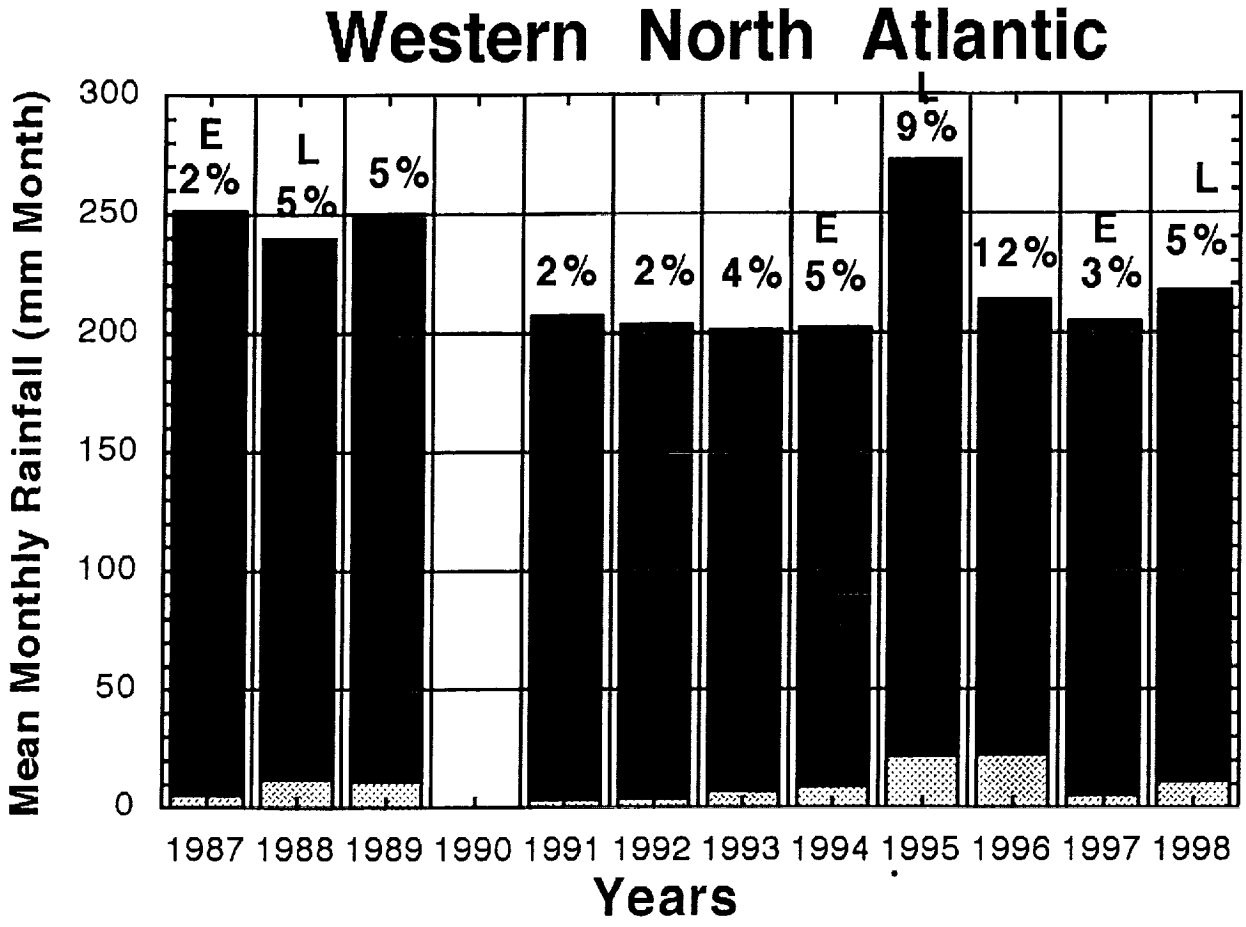
Western North Atlantic
Mean Monthly Rainfall (mm Month)
300
250
200
150
100
50
0
E 2%
L 5%
5%
2%
2%
4%
E 5%
L 9%
12%
E 3%
L 5%
1987 1988 1989 1990 1991 1992 1993 1994 1995 1996 1997 1998
Years

a

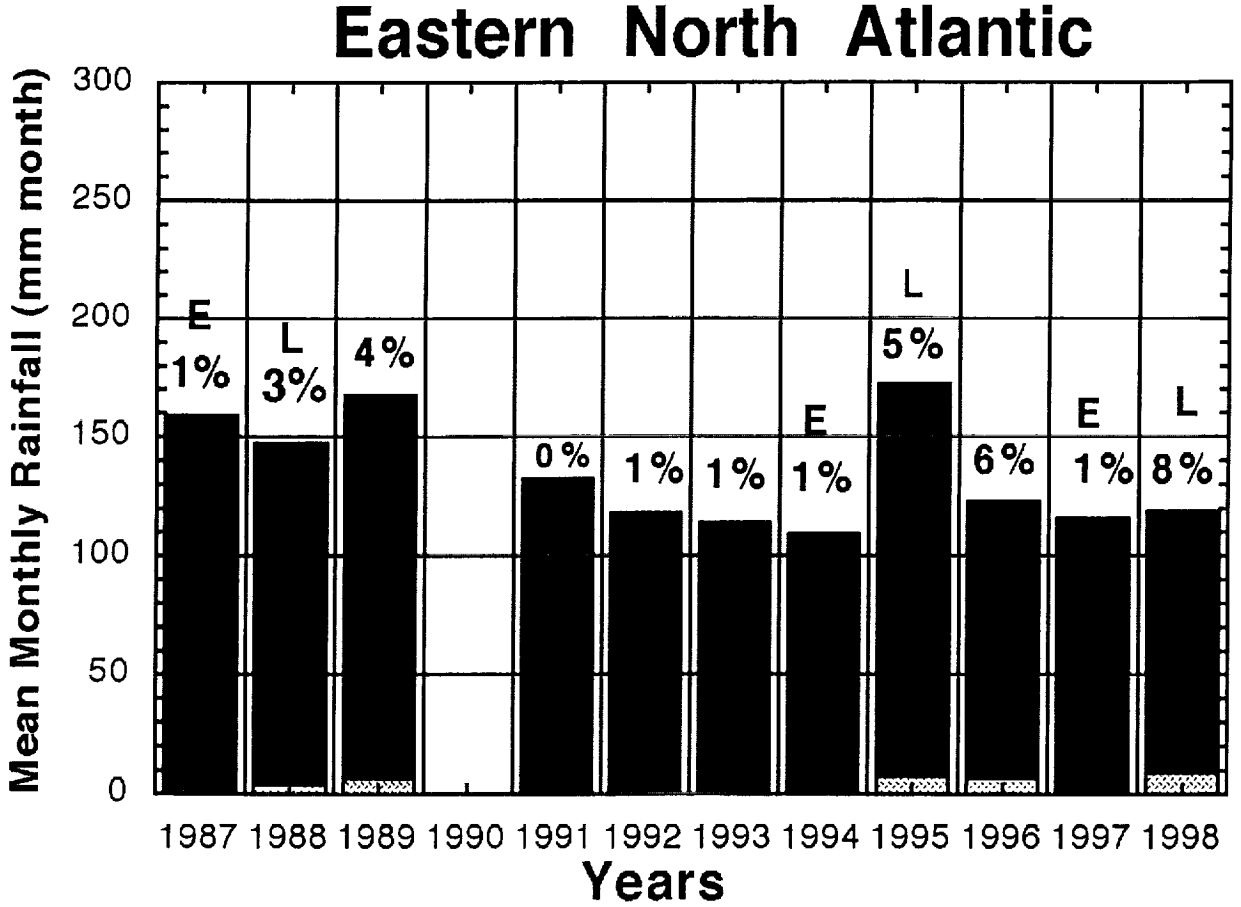
Eastern North Atlantic
Mean Monthly Rainfall (mm month)
300
250
200
150
100
50
0
E 1%
L 3%
4%
0%
1%
1%
E 1%
L 5%
6%
E 1%
L 8%
1987 1988 1989 1990 1991 1992 1993 1994 1995 1996 1997 1998
Years

b

Figure 11

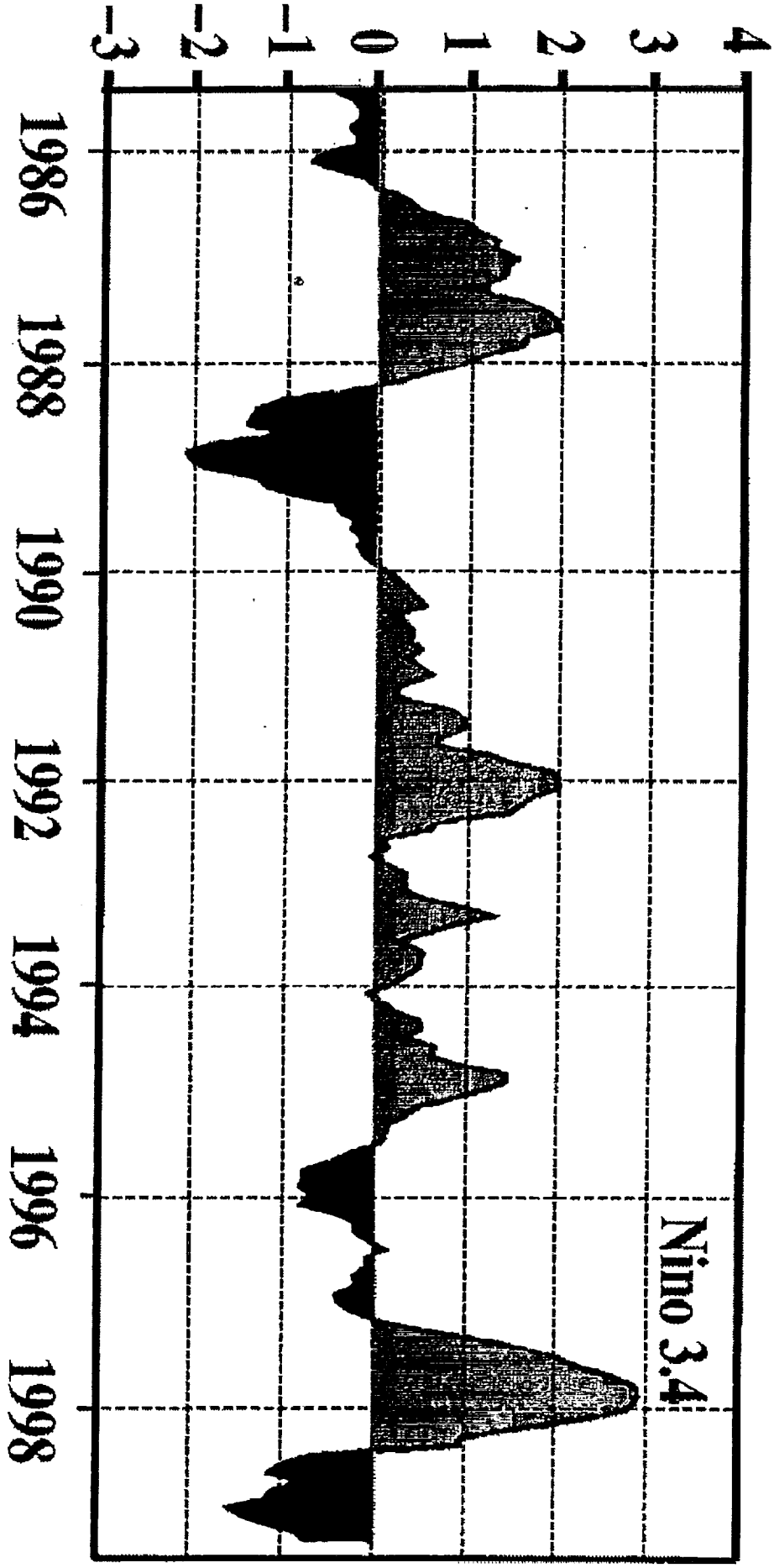

Figure 12

1987-1988 September SST Difference

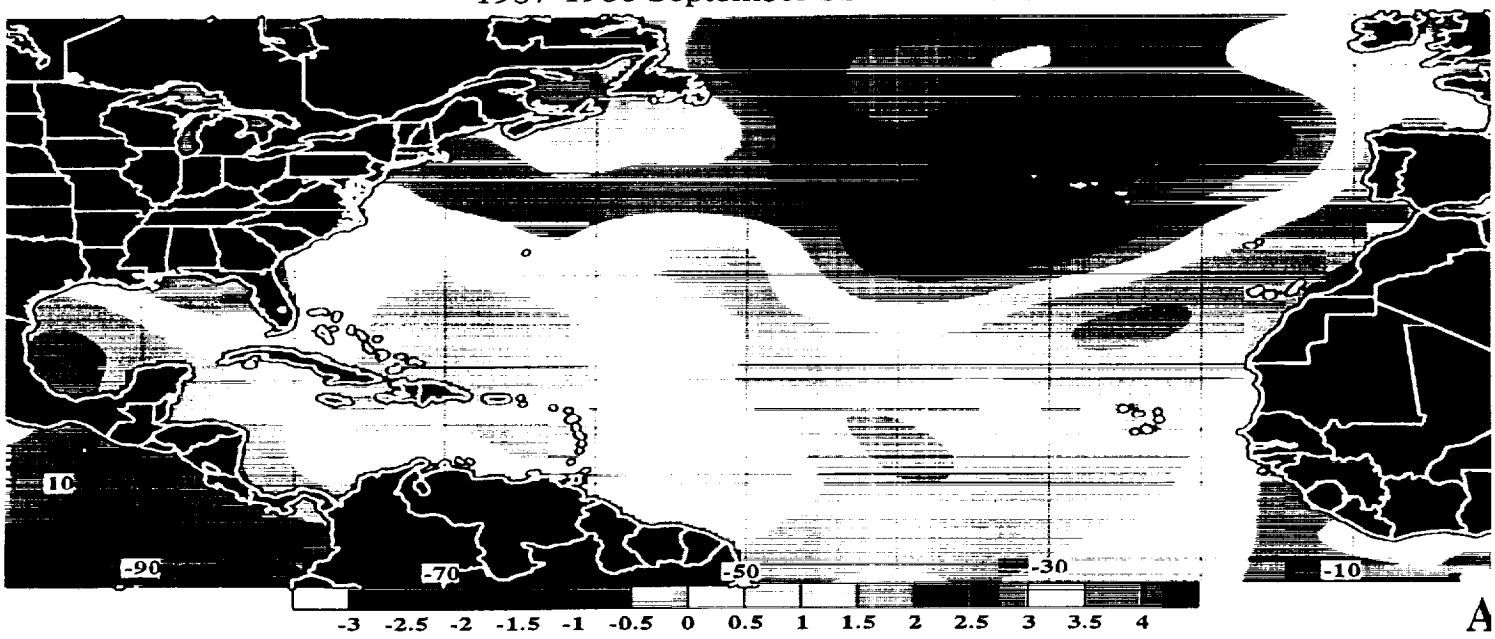

A

1994 - 1995 September SST Difference

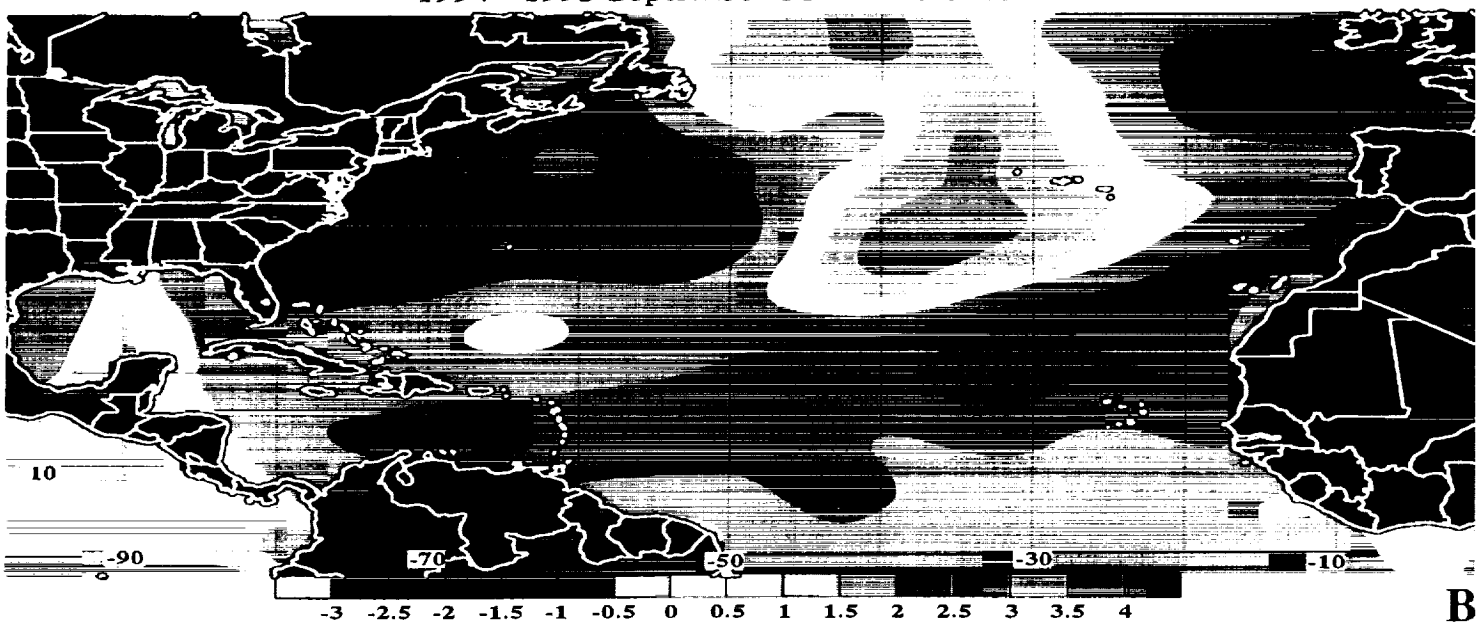

B

1997 - 1998 September SST Difference

Figure 13

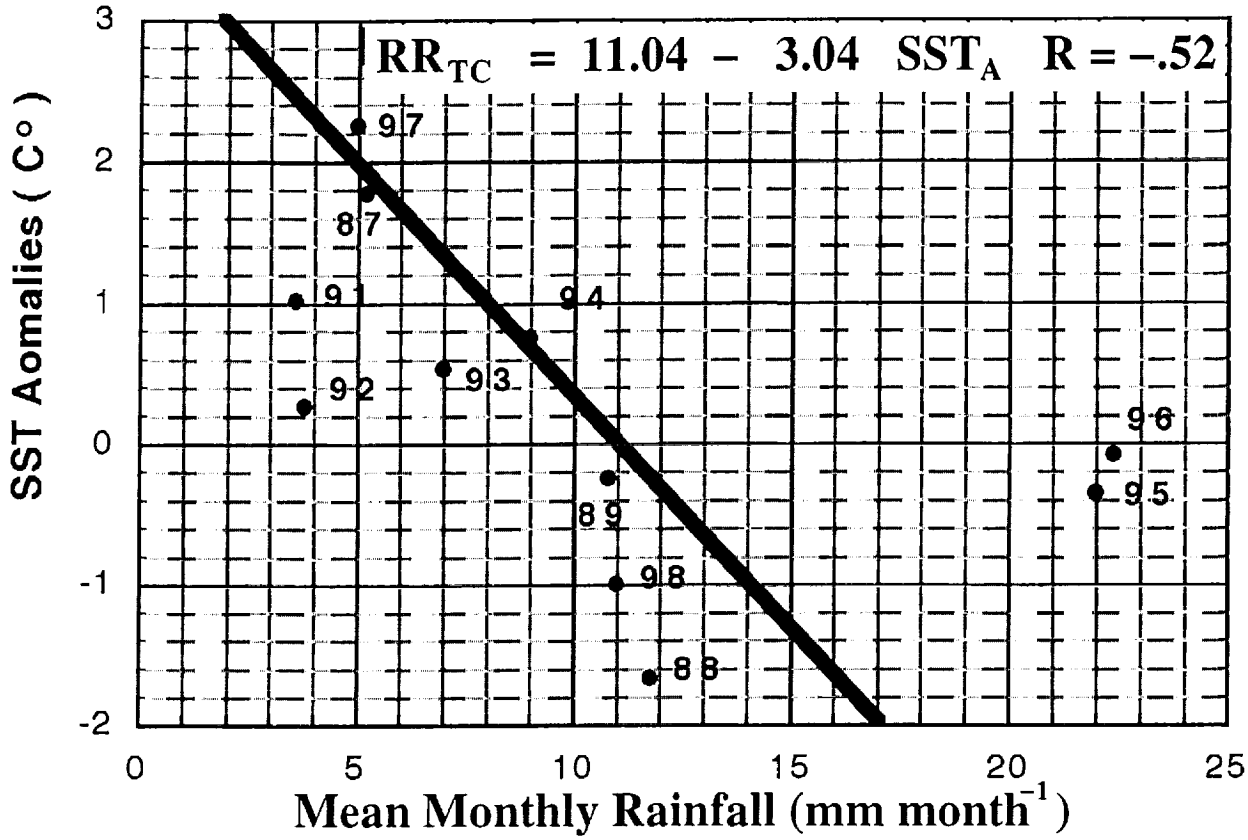
Western North Atlantic
RR_TC = 11.04 - 3.04 SST_A R = -.52
SST Aomalies (C°)
Mean Monthly Rainfall (mm month^-1)
97
87
91
94
92
93
96
95
89
98
88
3
2
1
0
-1
-2
0
5
10
15
20
25

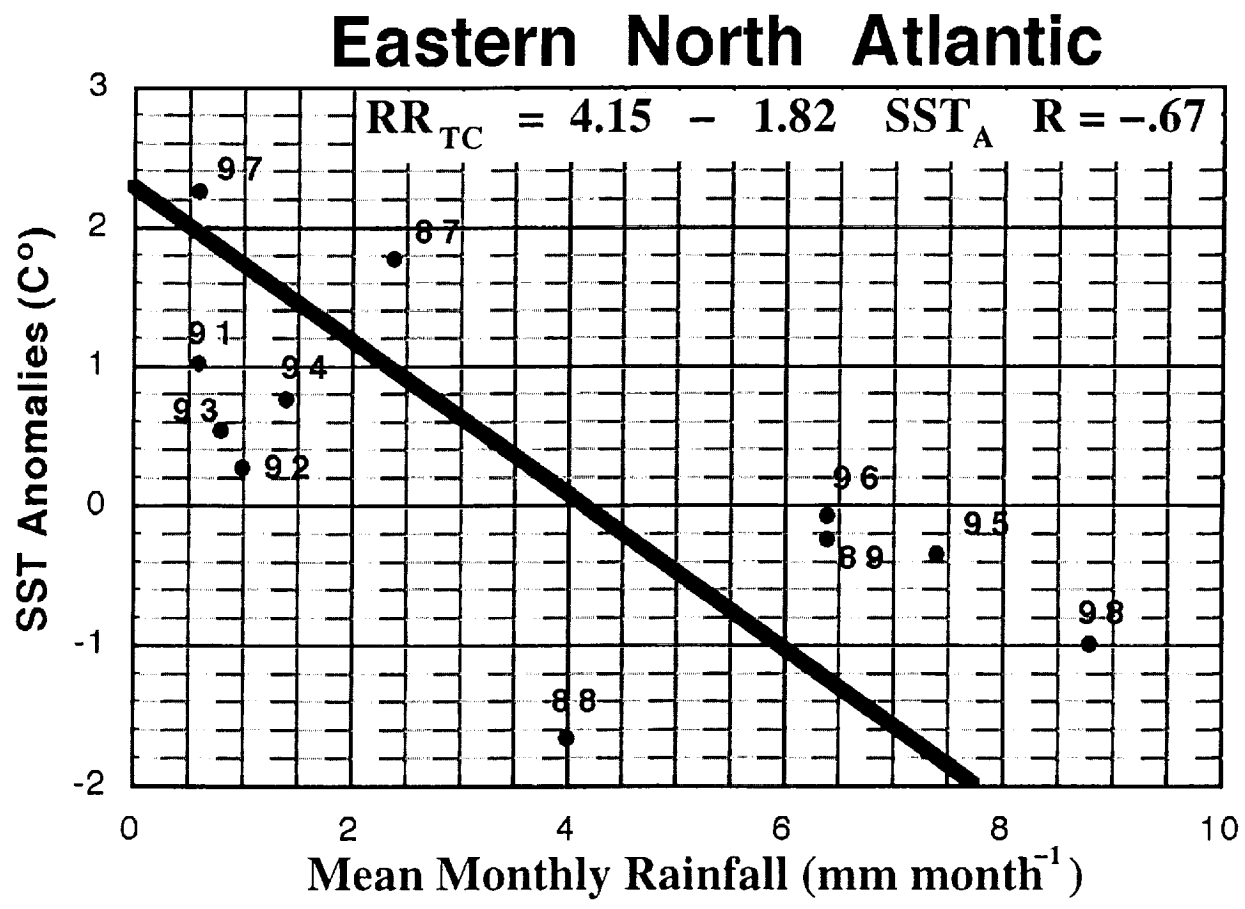
Eastern North Atlantic
RR_TC = 4.15 - 1.82 SST_A R = -.67
SST Anomalies (C°)
Mean Monthly Rainfall (mm month^-1)
97
87
91
94
93
92
96
95
89
98
88
3
2
1
0
-1
-2
0
2
4
6
8
10

Figure 14

Non-Tropical Cyclone Rain Difference (mm/mo) Between El Nino and La Nina Years

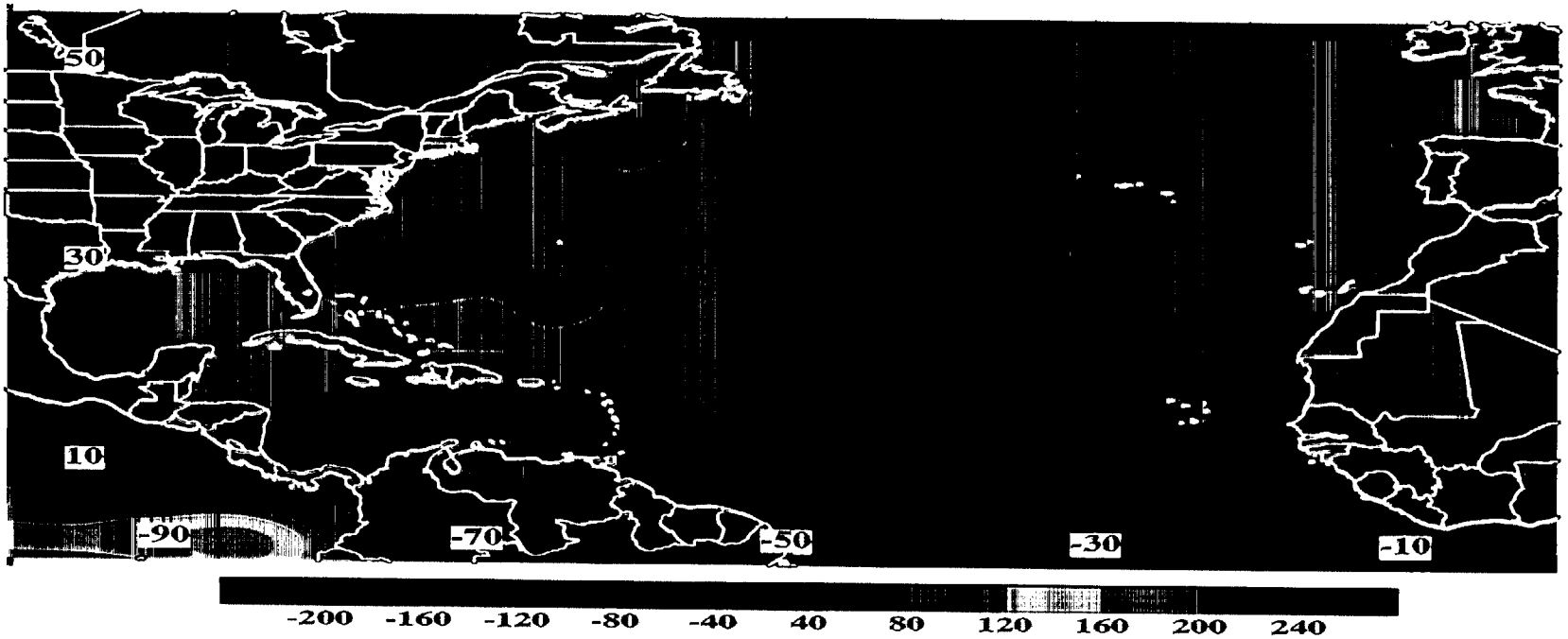

Tropical Cyclone Rain Difference (mm/mo) Between El Nino and La Nina Years

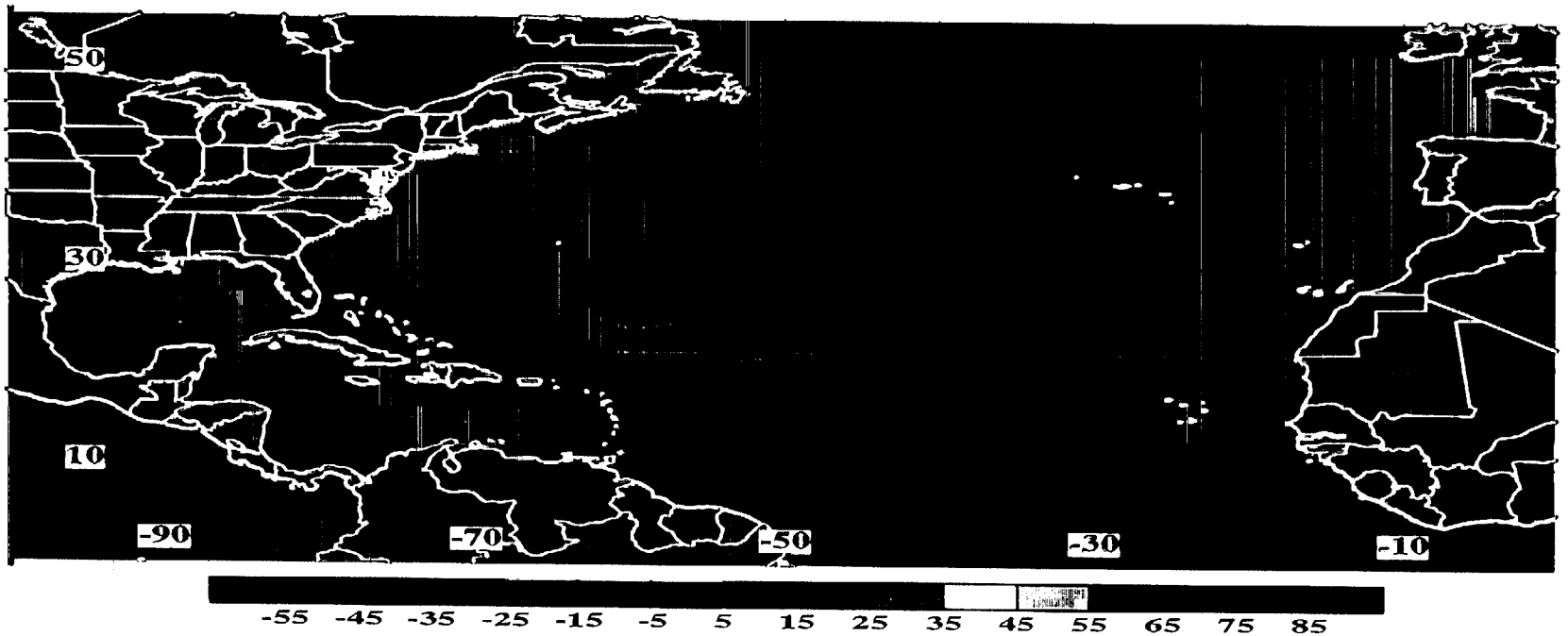

Figure 15

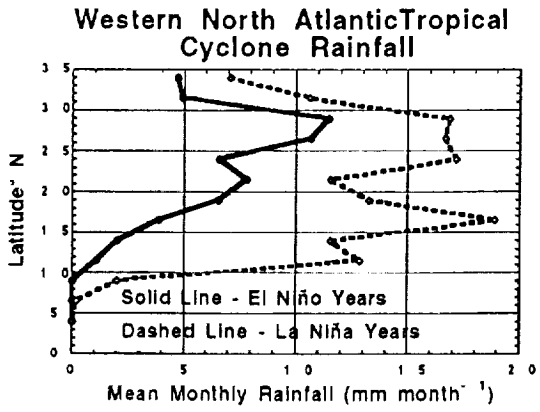

a

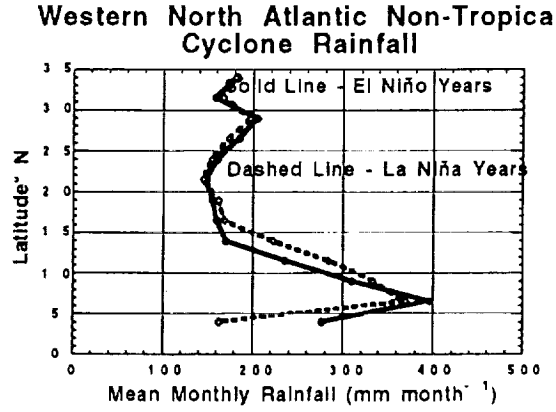

b

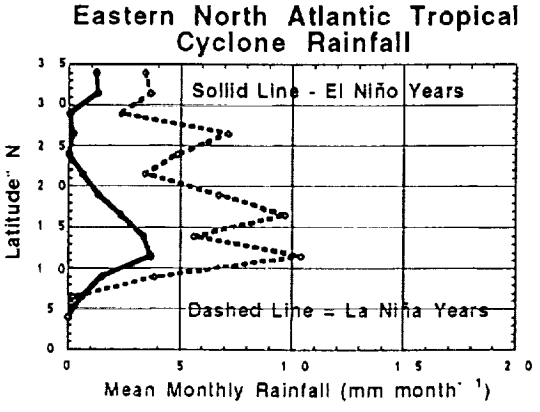

c

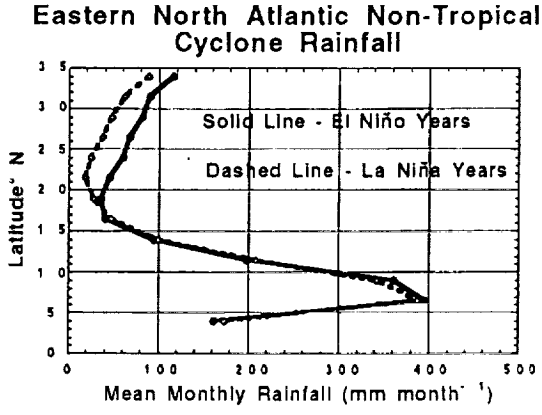

d

Figure 16